Neurobiology of Pain 16 (2024) 100160

Contents lists available at ScienceDirect

Neurobiology of Pain

journal homepage: www.sciencedirect.com/journal/neurobiology-of-pain

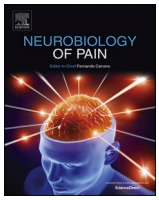

Adult zymosan re-exposure exacerbates the molecular alterations in the brainstem rostral ventromedial medulla of rats with early life zymosan-induced cystitis

Bhavana Talluri [a], Sankar Addya [b], Maia Terashvili [a], Bidyut K Medda [a], Anjishnu Banerjee [c], Reza Shaker [a], Jyoti N Sengupta [a], Banani Banerjee [a,*]

[a] Gastroenterology & Hepatology Division, Department of Medicine, Medical College of Wisconsin, Milwaukee, WI, USA
[b] Sydney Kimmel Cancer Center, Thomas Jefferson University, Philadelphia, PA, USA
[c] Division of Biostatistics, Medical College of Wisconsin, Milwaukee, WI, USA

ARTICLE INFO

Keywords:
Cystitis
Brainstem RVM
Synaptoneurosomes
Glutamatergic neurons
Synapse associated genes
microRNAs

ABSTRACT

Recent evidence suggests that the descending modulatory pathways from the brainstem rostral ventromedial medulla (RVM) are important for bladder inflammatory pain. This study aimed to identify the long-term molecular changes in RVM neurons due to early life cystitis during neuronal development and the effect of reexposure later in adulthood. RVM tissues from two treatment protocols were used: (1) neonatal zymosan exposures with acute adult rechallenge (RC) and (2) only neonatal zymosan exposures (NRC). RNAseq analysis showed upregulation of several genes associated with synaptic plasticity (Grin1, Grip2, Notch1, Arc, and Scn2b) in the cystitis groups compared to controls in both protocols. The RC protocol exhibited a stronger treatment effect with significantly higher fold differences between the groups compared to the NRC protocol ($p < 0.001$, fold differences RC vs NRC). In microarrays, miR-34a-5p showed cystitis-induced downregulation in both protocols. Bioinformatics analysis identified multiple 3′UTRs complementary binding sites for miR-34a-5p on Grin2b, Notch1, Grip2, Scn2b, and Arc genes. The enhanced response in the RC protocol indicates a possible priming effect of early life cystitis on rechallenge in adulthood. These long-term molecular alterations may play a critical role in the development of chronic bladder pain conditions as seen in patients with Interstitial Cystitis/Bladder pain syndrome.

1. Introduction

Interstitial cystitis and bladder pain syndrome (IC/BPS) are urological diseases which more commonly affect women than men, with a prevalence ranging from 2-6 % (Durden et al., 2018; Pierce & Christianson, 2015; Tirlapur et al., 2017). The etiology of IC/BPS is multifactorial and only incompletely understood. Possible pathologies include urothelial dysfunction, mast cell activation, genetic factors, autoimmunity, and central sensitization (Alagiri et al., 1997; Grundy et al., 2018; Offiah et al., 2022; Yang et al., 2021). Despite its high prevalence, the pharmacological treatment of bladder pain remains a significant challenge, and treatment outcomes are often unsatisfactory. Following the advent of molecular diagnostic treatment approaches, mechanism-based interventions have become widely accepted as specific and effective therapeutic strategies for treating various pain conditions (Cohen & Mao, 2014; Raja et al., 2019). The bladder is innervated by extrinsic afferents that provide sensory inputs to the spinal cord and supraspinal regions of the central nervous system (Grundy et al., 2018). There is increasing evidence to suggest that bladder pathophysiology may involve central sensitization with excitation of central pain signaling. As such, given the complex nature of bladder neurobiology, elucidation of the molecular alterations in the central pain modulatory system involved in the development and maintenance of chronic bladder pain associated with IC/BPS remains crucial.

The overall bladder nociceptive response comprises a complex sum of the excitatory and inhibitory processes at the peripheral and central levels (Grundy et al., 2018). The physiological and behavioral responses

Abbreviations: DEGs, Differentially expressed Genes; SYNs, Synaptoneurosomes; RC, Rechallenge; NRC, Nonrechallenge.

* Corresponding author at: Division of Gastroenterology and Hepatology, Medical College of Wisconsin, 8701 Watertown Plank Road, Milwaukee, WI 53226, USA.
E-mail address: banerjee@mcw.edu (B. Banerjee).

https://doi.org/10.1016/j.ynpai.2024.100160
Received 6 June 2024; Received in revised form 23 July 2024; Accepted 23 July 2024
Available online 24 July 2024

of animals to nociceptive stimuli have been shown to be either facilitatory or inhibitory, depending on the activation of separate subsets of neurons within the brainstem rostral ventromedial medulla (RVM) region. RVM neurons are the major targets of projections from the periaqueductal gray (PAG), the site of action of opioid-mediated analgesia (Basbaum & Fields, 1978; Heinricher et al., 2009; Ossipov et al., 2014; Peng et al., 2023). Prior studies have shown that the microinjection of NMDA (N-methyl-D-aspartate) receptor antagonists into the RVM results in attenuation of somatic and neuropathic pain implicating NMDA receptors in the facilitatory mechanisms of nociception within the RVM (Da Silva et al., 2010a; Da Silva et al., 2010b; Wei & Pertovaara, 1999). At the same time, RVM stimulations can cause inhibitory, facilitatory, and biphasic changes in the visceromotor responses (VMR) to graded urinary bladder distensions (UBD). The inhibitory response can be reduced by naloxone, suggesting the existence of a descending endogenous opioid inhibitory system. (Randich et al., 2008). However, experiencing bladder inflammation during the neonatal period impairs the expression of this opioid inhibitory mechanism in adulthood, suggesting that bladder insults during development may permanently alter visceral sensory systems and may represent one of the causes of BPS (DeBerry et al., 2007; Randich et al., 2008; Randich et al., 2006). Furthermore, experimental results indicate a significant priming effect of neonatal zymosan exposures on later life responses. The findings show that rats exposed to zymosan intravesically in early neonatal stages exhibited increased VMR when rechallenged with zymosan as adolescents. However, rats treated with the same exposures in adulthood did not show the same exaggerated VMR responses. This long-term sensitization from early life exposures may have clinical implications for patients with IC/BPS (DeBerry et al., 2007). To date, any plastic changes in the RVM neurons following induction of cystitis remain to be elucidated.

MicroRNAs (miRNAs) are small, noncoding RNA molecules that have recently emerged as major transcriptional regulators of gene expression. The identification of high expression of miRNAs in the nervous system has established their roles in dendritic morphogenesis, synaptogenesis, and synaptic plasticity (Lim et al., 2003; Pichardo-Casas et al., 2012; Williams et al., 2009; Zeng & Cullen, 2003). Several lines of evidence have implicated miRNAs in the pathophysiology of acute and chronic pain conditions (Niederberger et al., 2011). In line with these findings, we recently reported the involvement of miRNA-mediated post-transcriptional deregulation of spinal GABAergic neurons in rats with neonatally-induced cystitis (Sengupta et al., 2013; Zhang et al., 2017). These studies have established for the first time that the induction of cystitis during the developmental stage produces chronic visceral hyperalgesia due to an increase in spinal miR-181a and miR-92b-3p, with concomitant down-regulation of their target genes GABAA receptor subunit ($GABA_{A\alpha\text{-}1}$), Potassium chloride co-transporter (KCC2) and vesicular GABA transporter (VGAT), indicating an integral role for miRNA-mediated transcriptional deregulation of the spinal GABAergic neurotransmission in cystitis rats. As altered functions of RVM neurons contribute critically to the development of chronic pain, the identification of differentially expressed miRNAs and their target genes in the RVM may help to define the molecular mechanisms underlying cystitis-associated bladder pain.

Based on the existing literature and our previous findings, we aimed to investigate the effect of bladder zymosan exposures in rats during the early developmental phase and adulthood on the expression profiles of genes associated with glutamatergic neurotransmission in the RVM, and to determine whether miRNA-mediated transcriptional deregulation plays a role in the molecular alterations in RVM neurons following zymosan-induced cystitis. The findings of the study will facilitate the development of mechanism-based approaches for IC/BPS treatment.

2. Materials and methods

2.1. Animals

Female Sprague Dawley time-pregnant rats were purchased from Charles River Laboratories (Wilmington, MA, USA) and housed under controlled conditions with a 12-hour light–dark cycle and ad libitum access to food and water. All experiments were performed in accordance with the institutional guidelines and was approved by the Institutional Animal Care and Use Committee (IACUC) of the Medical College of Wisconsin (AUA 0355) and the International Association for the Study of Pain (IASP). The recommendations of the Office of Laboratory Animal Welfare (OLAW) were followed.

2.2. Treatment protocols

A schematic representation of the descending modulatory pathways from the midbrain to the spinal cord is shown in Fig. 1a. The interconnection between PAG-RVM-spinal cord pathways have been established as the predominant axis for the modulation of pain, while prior research has shown that the PAG sends direct synaptic projection to median RVM including nucleus raphe magnus (RMg) and nucleus gigantocellularis (NGc) (Heinricher et al., 2009). In this study, we investigated the molecular alterations in RVM neurons in zymosan-induced cystitis to decipher the intrinsic neuromolecular mechanisms underlying bladder pain syndrome. We used two treatment protocols: rechallenge (RC; Protocol 1) and non-rechallenge (NRC; Protocol 2), as shown in Fig. 1b. In all treatment protocols, the rats were anesthetized with isoflurane (1.5 % induction and 1.0 % maintenance at a flow rate of 1 L/min), as previously described (Kannampalli et al., 2017). In protocol 1 (RC), female pups received transurethral injections of protamine sulfate (1 % in saline, 0.1 ml), followed by transurethral zymosan (1 % in saline, 0.1 ml) from postnatal days 12 through 16 (P12 to P16). The protamine solution was left inside the bladder for 20 min after each injection prior to zymosan instillation. The pups in the control group received two doses of intravesical saline (0.1 mL) at similar intervals instead of protamine sulfate and zymosan following the same protocol as the experimental group. On postnatal day 29 (P29), the experimental group received an acute rechallenge with protamine sulfate (1 % in saline, 0.1 ml), followed by zymosan (1 % in saline, 0.1 ml), as described above, whereas the control group received two doses of saline (0.1 mL) at similar intervals. In protocol 2.(NRC), both the experimental and control groups received similar neonatal treatment as in protocol 1; however, the rats did not receive any rechallenge on P29. Brainstem RVM tissues were collected from both RC and NRC groups at P30.

2.3. Synaptoneurosomes (SYNs) isolation from RVM tissues

SYNs are biochemical preparations that retain large amounts of postsynaptic and presynaptic membrane components and synapse-associated proteins, making them useful for investigating the effects of treatments at the synaptic level (Banerjee et al., 2016; Johnson et al., 1997). We planned to study the synaptic alterations in the RVM following the induction of cystitis. On P30, rats were deeply anesthetized with sodium pentobarbital (60 mg/kg, i.p.), and RVM tissues were collected and resuspended in homogenization buffer. All subsequent steps were carried out on ice, as described previously (Banerjee et al., 2016; Johnson et al., 1997). Tissues were gently homogenized with 5–10 S of a loose pestle, followed by 5–10 S of a tight pestle, using a glass homogenizer (KIMBLE Dounce tissue grinder, Sigma Aldrich, St. Louis, MO). The homogenate was then centrifuged at 2000xg for 10 min. The supernatant was loaded into a 1 ml tuberculin syringe attached to a 13 mm diameter Millipore syringe filter holder carrying three 100 μm nylon filters (Millipore, Bedford, MA). Another set of filtrations using 5 μm pore PVDF syringe filters (Millipore) was performed, after which the isolated SYNs were further processed for total RNA isolation.

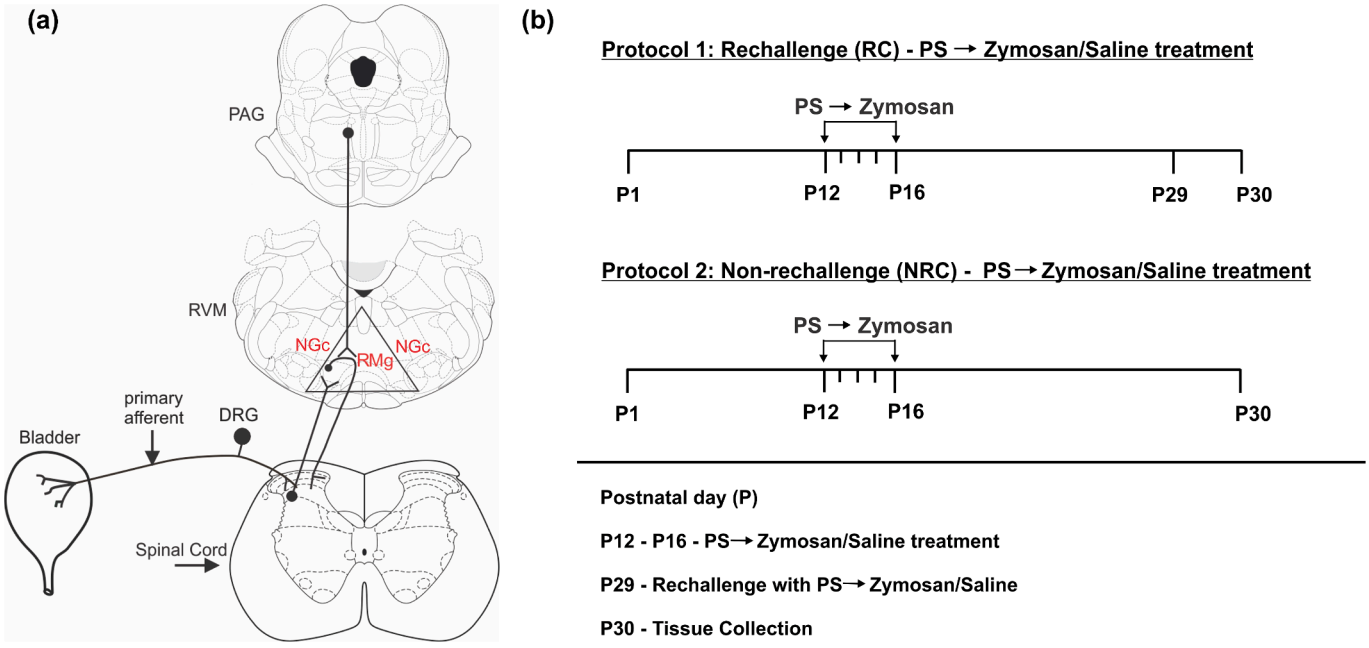

Fig. 1. Descending pain pathways and treatment protocols. A schematic representation of the descending modulatory (PAG-RVM-spinal cord axis) system contributing to hyperalgesia (**a**) and treatment protocols (**b**). The midline pain modulation center, PAG, transmits projections directly to the RVM. The RVM is defined as the midline pontomedullary area which includes the nucleus raphe magnus (RMg), nucleus gigantocellularis (NGc), and adjacent reticular formation. The RVM sends descending projections to the spinal dorsal horn laminae, including superficial layers and deep dorsal horn (**a**). Treatment protocols showing neonatal intraurethral instillation of protamine sulfate (PS)/saline + zymosan/saline followed by re-exposure at P29 for RC protocol and without any re-exposure for NRC protocols. RVM tissues were collected on P30 in both protocols (**b**).

2.4. Total RNA isolation from SYNs preparations

Total RNA was extracted from SYNs preparations using the Qiagen miRNeasy Mini Kit (Qiagen, Hilden, Germany), in accordance with the manufacturer's instructions. In brief, 400–500 μl QIAzol Lysis Reagent was added to the SYNs filtrate, and the homogenate was incubated at room temperature (15–25 °C) for 5 min. Subsequently, 200 μl chloroform was added to this mixture and shaken vigorously 15 times followed by centrifugation for 15 min at 12,000 x g at 4 °C. The upper aqueous phase was then collected and mixed with 100 % ethanol. The solution was then transferred into a RNeasy® Mini column and centrifuged to discard the flow-through. Following several wash steps, 30 μl of RNase free water was used to elute the total RNA from the RNeasy Mini column membrane. The total RNA concentration of each sample was measured using a NanoDrop spectrophotometer (Thermo Fisher Scientific, Waltham, MA, USA).

2.5. RNA-seq analysis of samples from RC and NRC treatment protocols

RNA-seq libraries for cystitis and control samples were prepared using Illumina standard total RNA prep ligation with the Ribo-Zero Plus Library Preparation Kit (Illumina, San Diego). The RNA libraries were sequenced on an Illumina NovaSeq 6000 instrument to generate 2 × 75 base-paired paired-end reads per sample and stored in the FASTQ format using Illumina's bcl2fastq converter. Paired-end sequence reads were analyzed in accordance with the current best practices for whole-transcriptome analysis, which included alignment onto the current rat reference genome assembly (rn6) using the STAR splice-aware aligner. Transcript abundance was estimated based on the current RefSeq gene annotations using the RSEM algorithm. Differential expression analysis was performed using DESeq2. For differentially expresses genes, a fold difference of 1.2-fold higher or lower between the groups with adjusted p values of $p \leq 0.1$ were considered significant. The experiments were performed at the Sydney Kimmel Cancer Center of Thomas Jefferson University (Philadelphia, PA, USA).

2.6. MicroRNA microarrays of samples from RC treatment protocol

Total RNA isolated from SYNs preparations of control and cystitis rats in the RC protocol was quantified using a NanoDrop ND-1000 spectrophotometer, and RNA quality was assessed using an Agilent 2100 Bioanalyzer (Agilent, Palo Alto, CA, USA). RNA labeling was performed using the FlashTag Biotin RNA Labeling Kit from Affymetrix GeneChip miRNA Arrays (Genisphere, Hatfield, PA, USA). Affymetrix® GeneChip® miRNA Arrays (Affymetrix, Santa Clara, CA) were hybridized with Flash Tag Biotin Labeled total RNA from experimental and control samples in 100 μl hybridization cocktail. Target denaturation and hybridization were performed in accordance with the manufacturer's instructions. The arrays were then washed and stained using GeneChip Fluidic Station 450, and hybridization signals were amplified using antibody amplification with goat IgG (Sigma-Aldrich) and anti-streptavidin biotinylated antibody (Vector Laboratories, Burlingame, CA, USA). Chips were scanned on an Affymetrix Gene Chip Scanner 3000 using the Command Console Software. The miRNA data were analyzed using the Affymetrix miRNA QC tool. The raw data were normalized and analyzed using GeneSpring software version 7.2 (Silico Genetics, Redwood, CA, USA). To identify differentially expressed miRNAs in cystitis rats, the ratio of expression in each cystitis rat to the average expression in all controls was calculated for each miRNA. Expression signals were normalized to average median of all miRNAs in the array and miRNAs with 1.4-fold higher or lower expression compared to average value in the control animals were selected for further analysis. Background correction and normalization were carried out using Robust Multichip Average (RMA) with GeneSpring software (version 10.0; Agilent, Palo Alto, CA, USA). This study was conducted at the Sydney Kimmel Cancer Center of Thomas Jefferson University, Philadelphia, USA.

2.7. IPA analysis for differentially expressed genes (DEGs) and miRNAs

Ingenuity Pathway Analysis (IPA) system was applied for subsequent

bioinformatic analysis, which included canonical pathway analysis, diseases, and functions, using software from Qiagen (QIAGEN Inc., https://www.qiagenbioinformatics.com/products/ingenuity) by loading normalized sequencing read sets for selected DEGs in both the RC and NRC protocols. The -log (P-value) > 2 was taken as threshold, and a Z-score > 2 was defined as the threshold of significant activation, whilst a Z-score <-2 was defined as the threshold of significant inhibition. Differentially expressed miRNAs were subjected to disease/function analyses using the IPA system.

2.8. Target gene prediction for differentially expressed miR-34a-5p

The target gene predications with complementary binding sites for the miR-34a-5p seed region were analyzed using a combination of several Bioinformatic algorithms including MiRWalk, MicroT4, MiRanda, mirbridge, MiRDB, MiRMap, miRNAMap, Pictar 2, PITA, RNA22, RNAhybrid & TargetScan (Dweep & Gretz, 2015; Kern et al., 2021; Zhang et al., 2017).

2.9. Validation of selected genes found to be differentially expressed in the RC protocol using TaqMan Real Time-PCR

Total RNAs from RVM tissues of saline- and cystitis-treated rats were subjected to reverse transcription using the High-Capacity cDNA Reverse Transcription Kit (Invitrogen). RT-PCR was performed using TaqMan Gene Expression Assays (FAM) and TaqMan Fast Advanced Master Mix (Thermo Fisher Scientific). Differentially expressed genes were normalized against housekeeping 18S rRNA and the relative expression of each gene was determined as $2_{T}^{-[C_{T}^{miRNA-CrRNA}]}$. Relative fold-change ($Log_2$ FC) was calculated for differentially expressed genes in the cystitis group compared to the saline controls. The PCR reactions were carried out using the QuantStudio™ 6 Pro Real-Time PCR System (Thermo Fisher Scientific).

2.10. Validation of differentially expressed miR-34-5p in RC protocol using TaqMan RT-PCR

Total RNA from RVM tissues of saline and cystitis rats were reverse transcribed using TaqMan™ Advanced miRNA cDNA Synthesis Kit (Thermo Fisher Scientific). The final cDNA template was further diluted 1:10 in TE buffer, as described in the manufacturer's protocol. RT-PCR was performed using TaqMan Advanced miRNA Assays and TaqMan Fast Advanced Master Mix (Thermo Fisher Scientific). miR-34a-5p expression was normalized against miR-93-5p and represented as $2_{T}^{-[C_{T}^{miR\text{-}34a\text{-}5p-C\,miR\text{-}93\text{-}5p]}}$. PCR reactions were performed in duplicate, and No Target Control (NTC) was used as a negative control. The PCR reactions were carried out in a QuantStudio™ 6 Pro Real-Time PCR System (Thermo Fisher Scientific).

2.11. Dual in situ hybridization (ISH) / immunohistochemistry (IHC) analysis of miR-34a-5p expression and its target genes NR2B, Notch1, and Arc in RVM neurons

In situ hybridization chain reaction (HCR) was performed to identify miRNAs in tissue sections along with combined antibody staining, as described previously (Zhuang et al., 2020). We chose mid-level RVM tissue sections (bregma: −11.8 mm) for analysis based on our recent observation, which indicated a higher innervation of bladder-linked neurons into the mid-level compared to the rostral and caudal levels of the RVM [31]. In brief, RVM tissue sections from naïve rats were mounted onto Fisherbrand™ Superfrost™ Plus Microscope slides and incubated at 37 °C for 30 mins. The slides were post-fixed in 4 % PFA for 20 min at room temperature and washed twice with PBS for 5 min each. Tissue sections were treated with 10 μg/ml Proteinase K for 6 min and washed in PBS for 10 mins. Slides were fixed in 4 % PFA for 15 min, and washed twice in PBS for 5 min each, followed by a brief wash in ultrapure water. The slides were then incubated in 0.1 M Triethanolamine and acetic anhydride for 5 min and washed in PBS for 10 min. The tissues were pre-hybridized with hybridization solution (15 % formamide; 5X SSC; 0.3 mg/ml yeast RNA; 100 μg/ml Heparin; 1X Denhardt's solution; 0.1 % Tween 20; 0.1 % CHAPS; 5 mM EDTA and 3 μl/ml random primer in 50 ml of RNase-free Ultrapure water) without probe for 2.5 h at 37 °C. A final concentration of 20 pmol of miR-34a-5p and negative control probes were added to 200 μl hybridization solution and the slides were incubated overnight at 37 °C for 18 h. The probe sequences were as follows: miR-34a-5p- 5′-CTC TAT ATC TCC AAC CCG AAA CAA CCA GCT AAG ACA CTG CAA TAA TCC CTC TAT ATC TCC-3.' Negative control: 5′-CTC TAT ATC TCC AAC CCG TTC CTA TAG GAC TAT CCA GGA ATT TAA TCC CTC TAT ATC TCC-3′. The following day, slides were subjected to high stringency washing with TMAC at 45 °C for 30 min. The slides were then pre-amplified in amplification buffer for 30 mins followed by incubation with 12 pmol/200 μl of hairpin amplifier for 2 h. The slides were then washed with 5X SSCT three times for 10 min each, followed by incubation in blocking solution for 1 h. The slides were incubated with the primary antibody for 2 h, followed by incubation with the secondary antibody for 1 h. Finally, the tissues were washed and mounted using a mounting solution containing DAPI. The staining was visualized and imaged using a fluorescence microscope (Nikon Eclipse 50i; Nikon, Tokyo, Japan). High-magnification images were captured on a confocal microscope (Nikon A1-R, Tokyo, Japan) using blue/DAPI and green and red channels under similar settings of exposure, gain, and gamma adjustment at 60X magnification.

2.12. IHC analysis of the NR2B, Notch1, and Arc expression in RVM glutamatergic neurons

RVM mid-level tissue sections of naïve rats (n = 3) were used for IHC analysis The floating RVM sections were subjected to antigen retrieval with target retrieval solution (Dako, Santa Clara, CA) for 30 min at 80 °C. The tissue sections were washed and incubated in blocking buffer containing 10 % NGS in PBS for 2 h at room temperature. Tissue sections were then incubated with primary antibodies Mouse Anti-NMDAR1 (1:250, BD Pharmingen™, Franklin Lakes, NJ) along with either, Rabbit Anti-NMDAR2B (1:250, Alomone Labs, Jerusalem, Israel) or Rabbit Anti-Notch1 (1:500, Thermo Fisher Scientific) or Rabbit anti-Arc (Synaptic Systems, Göttingen, Germany) in 5 % NGS overnight at 4 °C with gentle shaking. The following day, tissue sections were washed and incubated with Alexa Fluor 488 goat anti-mouse and Alexa Fluor 568 goat anti-rabbit secondary antibodies for 2 h at room temperature. Finally, the tissue sections were washed and mounted on slides for visualization under a fluorescence microscope (Nikon Eclipse 50i; Nikon, Tokyo, Japan) using red and green fluorescence filters. NR1 positive neurons were identified in the green channel, while NR2B-, Notch1, and Arc-positive neurons were identified in the red channel in the same tissue section. Images were captured under individual fluorescence channels, and co-localized neurons were identified by merging images taken with independent filters. All cells exhibiting green, red, and/or merged fluorescence were counted using the ImageJ software (NIH, Bethesda, MD, USA).

2.13. IHC analysis of the effect of cystitis on NMDA subunits NR1 and NR2B expression in RVM neurons in RC protocol

RVM tissues sections from both neonatal cystitis and saline-treated rats (n = 3/group) were subjected to antigen retrieval at 80 °C for 30 mins. Tissue sections were subsequently blocked and incubated with primary antibodies Mouse Anti-NMDAR1 (1:250, BD Pharmingen™) and Rabbit Anti-NMDAR2B (1:250, Alomone Labs) overnight. The following day, the tissue sections were washed and incubated with secondary antibodies: Alexa Fluor 488 goat anti-mouse and Alexa Fluor 568 goat anti-rabbit. Staining intensity was examined using a fluorescence microscope (Nikon Eclipse 50i, Nikon) and a confocal microscope (Nikon A1-R, Nikon). For quantification, the images were converted to

grey scale, and the intensity of immunostaining in the neuron was measured by drawing around the cell/neuron to measure the region of interest (ROI (Image J, NIH Bethesda)). We selected the region next to the ROI with no fluorescence to measure the background. For each selected field, we measured the background near the ROI, and used the average to calculate the Corrected Total Cell Fluorescence (CTCF). Data analysis was performed to compare the CTCF of NR2B and NR1 expression in saline- and zymosan-treated rats, defined as CTCF=Integrated Density – (area of selected cell × mean fluorescence of background readings). The intensities of NR1 and NR2B immunostaining were measured using ROIs of 3–5 cells in each tissue section. The mean CTCF was measured in three sections per animal (n = 3/group).

2.14. Data analysis

All images were edited and compiled using Adobe Photoshop CS6 (version 13.0) and CorelDRAW X8 (version 18.1) software. Statistical analyses were performed using GraphPad Prism (version 10). Statistical differences in fold changes between the treatment protocols (RC and NRC) and regulation type (up and down) were examined using a multivariable regression model in R studio (Version 4.4.0). We compared the fold change between RC and NRC treatment protocols, with $p < 0.05$ indicating statistical significance. For IHC analysis, an unpaired *t*-test with Welch's correction was used to compare data between the cystitis and control groups using the GraphPad Prism software. Data represented as the average CTCF ± SD, with $p \leq 0.05$ vs controls considered significant.

3. Results

3.1. Upregulation of genes associated with glutamatergic neurotransmission in RVM SYNs of neonatal cystitis rats with acute adult rechallenge in the RC protocol

We performed RNA-seq analysis of RVM SYNs preparations from the cystitis and control rats. Among the differentially expressed genes, 60 associated with synaptic plasticity and glutamatergic neurotransmission with ≥ 1.5-fold change, $p < 0.05$, adjusted $p \leq 0.1$ cystitis vs controls, were selected for further analysis (Fig. 2a-d, Supplementary Table S1). The overall gene expression profiles from the RNA-seq analysis are shown in Supplementary Table S2. We evaluated the effects of neonatal zymosan treatment with acute adult rechallenge on the expression of several receptors, enzymes, and transporters involved in glutamatergic neurotransmission in RVM SYNs from cystitis and control rats (Fig. 2a). Major postsynaptic ionotropic glutamate NMDA receptor subtypes, Grin1 (NR1,1.8-fold vs controls), Grin2A-2D (NR2A-2D,1.5 to 2-fold vs. controls), and Grin3A (1.7-fold vs. controls), demonstrated a significant increase in cystitis rats compared to saline controls. The gene encoding glutamate receptor interacting protein 2 (Grip2), a positive regulator of excitatory postsynaptic potential, further exhibited > 3-fold upregulation in the experimental group compared to controls (Fig. 2a). Among the differentially expressed synapse-associated proteins, the expression

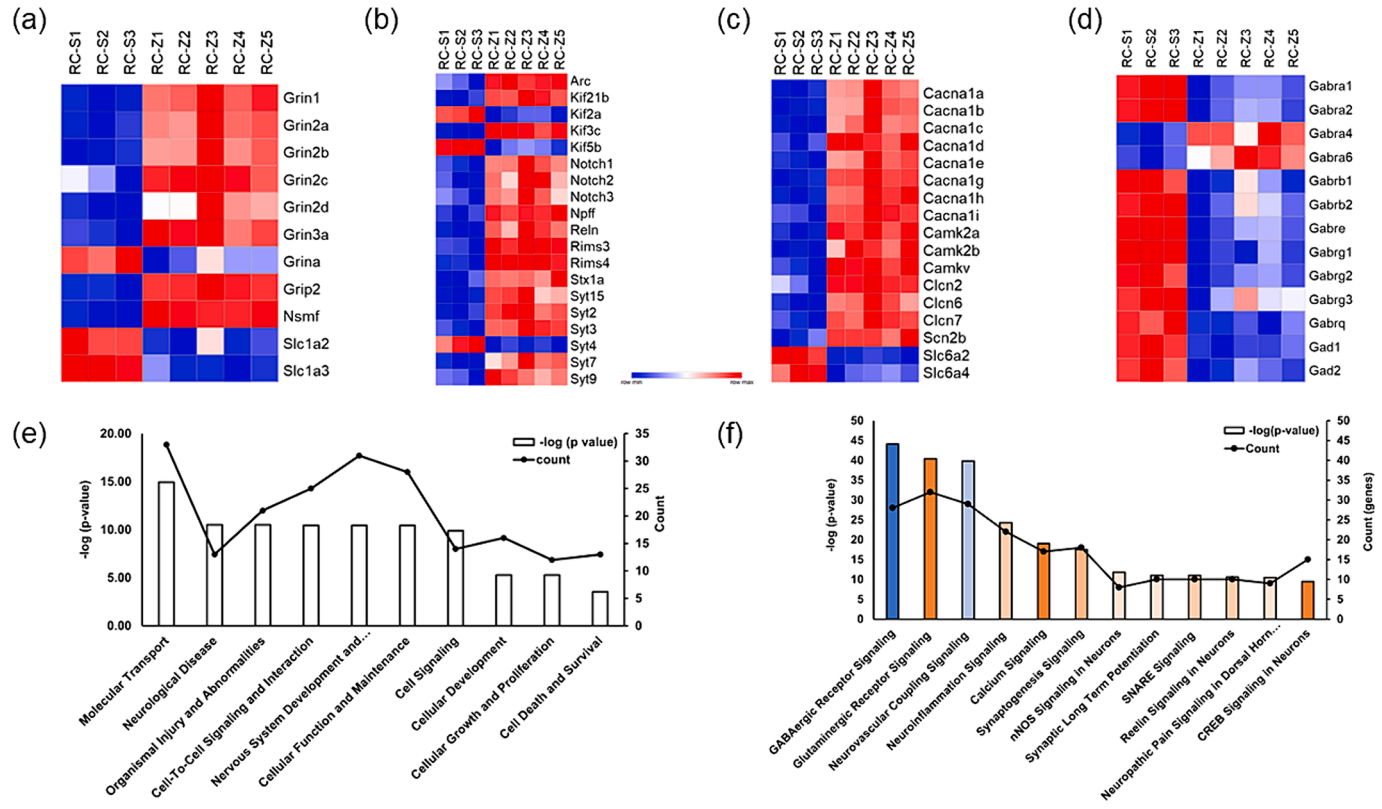

Fig. 2. RNAseq analysis of RVM tissues from RC protocol 1. Heat Maps of the 60 selected genes associated with glutamatergic neurotransmission and synaptic plasticity which were differentially expressed in RVM SYNs preparations from cystitis rats (n = 5) compared to controls (n = 3) (≥1.5-fold difference, $p \leq 0.05$ and adjusted $p \leq 0.1$ vs controls). Genes associated with the Glutamatergic pathway (**a**), synaptic plasticity (**b**), voltage-gated calcium and sodium channels signaling (**c**), and the GABAergic pathway (**d**). Histogram of IPA analysis of the selected DEGs showing involvement in 10 diseases and functions (**e**). The left y–axis represents the –log (p–value) and the right y–axis represents the number of genes involved in each disease/function. The threshold for the selection of the pathways were set as –log (P–value) ≥ 2 or ≤ -2. A Z–score ≥ 2 represents the threshold of significant activation, and Z–score ≤ –2 defines the threshold of significant inhibition. Histogram of IPA analysis showing 12 canonical pathways (**f**). The left y–axis represents the –log (p–value), and the right y–axis represents the number of genes involved in each representative canonical pathway. A Z–score ≥ 2 represents the threshold of significant activation, and a Z–score ≤ –2 defines the threshold of significant inhibition. In the plotted histograms higher Z-scores (shown in orange) indicate activation, whilst lower Z-scores (shown in blue) indicate inhibition of the pathways. (For interpretation of the references to colour in this figure legend, the reader is referred to the web version of this article.)

levels of Notch1, Notch2, and Notch3 were significantly higher in rats with cystitis (>1.7-fold vs. controls; (Fig. 2b)). A recent study indicated the functional interaction between post-synaptic Notch1 and NMDA receptors in hippocampal neurons, while the loss of Notch1 was reported to affect the expression and composition of NMDA receptors at the synapses (Brai et al., 2015). Simultaneously, the activity-related plasticity gene (Arc/Arg3.1), a positive regulator of neuronal Notch signaling, further exhibited a significant increase in RVM neurons following zymosan treatment (Fig. 2b). Similarly, synaptic vesicles syntaxin1a, syt2, syt3, syt7, and syt9, which interact directly or indirectly with voltage-gated calcium channels (VGCCs) and regulate their function within the presynaptic terminal, also exhibited significant upregulation in zymosan-treated rats (Fig. 2b). Genes encoding the active zone proteins RIMS3 and RIMS4 were significantly upregulated (>2-to 4-fold vs. controls; (Fig. 2b)) in the cystitis group following zymosan rechallenge later in life. These active zone proteins are expressed in glutamatergic synapses and are involved in the calcium ion-regulated exocytosis of neurotransmitters.

3.2. Differential expression of presynaptic VGCCs and voltage-gated sodium channel (Scn2b) in the RVM neurons of cystitis rats in the RC protocol

RNA-seq analysis further revealed the upregulation of several members of the VGCCs cluster, including Cacna1a (Cav2.1), Cacna1b (Cav2.2), Cacna1g (Cav3.1), Cacna1h (Cav3.2), and Cacna1i (Cav3.3), in RVM neurons of zymosan-treated rats compared to saline controls (>1.5-fold vs. controls, (Fig. 2c)). The pain-relevant sodium channel Scn2b was also significantly upregulated in cystitis rats compared with controls (>1.7-fold vs. controls, (Fig. 2c)). These findings indicate that the increase in the expression of various VGCCs and related vesicular and active zone proteins in rats with neonatal cystitis following adult rechallenge may profoundly influence the strength of neurotransmitter output at glutamatergic synapses.

3.3. Downregulation of receptors/enzymes associated with GABAergic signaling in RVM SYNs of cystitis rats in the RC protocol

GABA is a widely distributed inhibitory neurotransmitter in the CNS; an estimated 20–50 % of central synapses express ionotropic GABAA receptors (Fritschy & Brunig, 2003). Multiple studies suggest that the majority of GABAA receptors in the brain are composed of the subunits α1, β2, and γ2. Our RNA-seq analysis further revealed a significant downregulation of these subunits in cystitis rats, indicating an underlying GABAergic disinhibition in RVM neurons in zymosan rechallenge neonatal cystitis rats (Fig. 2d). Moreover, there was a decrease in Gad1 and Gad2, enzymes involved in GABA synthesis, in rats with cystitis (>1.5-fold, vs. controls).

3.4. IPA analysis of the differentially expressed genes in disease/function and canonical pathways

Sixty selected DEGs involved in synaptic processing were subjected to IPA (version 42012434, Ingenuity Systems; Qiagen), and subsequent bioinformatics analyses to identify their involvement in various diseases/functions and canonical pathways. Our data indicated that several functions and diseases, including cellular function and development, cell-to-cell interactions, neurological diseases, and molecular transport, were significantly activated following cystitis compared to saline controls (Fig. 2e, Table 1). The number of DEGs involved in disease and function ranged from 10 to 35 (Table 1). Additionally, IPA analysis demonstrated a significant downregulation of GABAergic receptor signaling pathway in cystitis rats (Fig. 2f, Z scores ≤ -2.0; Supplementary Table S3) with concomitant activation of several excitatory pathways including glutaminergic, calcium signaling, neuroinflammatory and synapse associated signaling (Fig. 2f, Z-score ≥ 2.0).

Table 1
IPA analysis of DEGs for diseases and functions.

Category	p-value	-log (p value)	Genes
Molecular Transport	1.14E-15	14.94	ARC,CACNA1A,CACNA1B, CACNA1C,CACNA1D,CACNA1E, CACNA1G,CACNA1H,CACNA1I, CAMK2A,CLCN2,GABRB1, GABRB2,GABRE,GABRG2,GAD2, GRIN1,GRIN2A,GRIN2B, GRIN2D,GRIN3A,RIMS3,RIMS4, SLC1A2,SLC1A3,SLC6A2, SLC6A4,STX1A,SYT2,SYT3,SYT4, Syt7,SYT9
Neurological Disease	3.10E-11	10.51	ARC,CACNA1B,CACNA1C, CAMK2A,GAD1,GAD2,GRIN1, GRIN2A,GRIN2B,GRIN2D, GRIN3A,SLC1A2,SLC1A3
Organismal Injury and Abnormalities	3.10E-11	10.51	ARC,CACNA1A,CACNA1B, CACNA1C,CACNA1G,CACNA1H, CAMK2A,CAMK2B,CLCN6,GAD1, GAD2,GRIN1,GRIN2A,GRIN2B, GRIN2D,GRIN3A,NOTCH1, NOTCH3,NSMF,SLC1A2,SLC1A3
Cell-To-Cell Signaling and Interaction	3.65E-11	10.44	ARC,CACNA1A,CACNA1B, CAMK2A,CAMK2B,GABRA1, GABRG2,GAD1,GAD2,GRIN1, GRIN2A,GRIN2B,GRIN2C, GRIN2D,GRIP2,NPFF,NSMF, RIMS3,RIMS4,SLC1A2,SLC1A3, SLC6A2,SLC6A4,STX1A,SYT4
Nervous System Development and Function	3.65E-11	10.44	ARC,CACNA1A,CACNA1B, CACNA1E,CACNA1H,CAMK2A, CAMK2B,GABRA1,GABRG2, GAD2,GRIN1,GRIN2A,GRIN2B, GRIN2C,GRIN2D,GRIN3A,GRIP2, KIF2A,KIF3C,NOTCH1,NOTCH3, NPFF,NSMF,RELN,RIMS3,RIMS4, SLC6A4,STX1A,SYT2,SYT3,Syt7
Cellular Function and Maintenance	3.66E-11	10.44	ARC,CACNA1C,CACNA1D, CACNA1E,CACNA1G,CACNA1H, CACNA1I,CAMK2A,CAMK2B, CLCN2,GABRB2,GABRG2,GRIN1, GRIN2A,GRIN2B,GRIN3A,KIF3C, NOTCH1,NPFF,NSMF,RIMS3, RIMS4,SLC6A4,STX1A,SYT2, SYT3,Syt7,SYT9
Cell Signaling	1.29E-10	9.89	ARC,CACNA1A,CACNA1B, CACNA1C,CACNA1D,CACNA1G, CACNA1H,CACNA1I,CAMK2A, GRIN1,GRIN2B,GRIN3A,NPFF, SLC6A4
Cellular Development	5.12E-06	5.29	ARC,CAMK2A,CAMK2B,GRIN2B, GRIN3A,GRIP2,KIF2A,KIF3C, NOTCH1,NOTCH2,NOTCH3, NSMF,RELN,RIMS3,RIMS4, SLC6A4
Cellular Growth and Proliferation	5.12E-06	5.29	ARC,CAMK2A,CAMK2B,GRIN2B, GRIN3A,KIF2A,KIF3C,NOTCH1, NSMF,RELN,RIMS3,RIMS4
Cell Death and Survival	2.97E-04	3.53	CACNA1A,CACNA1G,CACNA1H, CAMK2A,CAMK2B,GAD2,GRIN1, GRIN2A,GRIN2B,NOTCH1, NSMF,SLC1A2,Syt7

3.5. Zymosan rechallenge in adulthood exacerbates the underlying molecular alterations in RVM neurons of rats with zymosan-induced neonatal cystitis

We intended to examine whether neonatal cystitis/bladder inflammation exerts a long-term effect on molecular expression in RVM neurons and whether there is an exacerbation of the underlying molecular alterations when rats with neonatal cystitis receive zymosan re-exposure later in adulthood. The RVM samples from the NRC rats in protocol 2, as described in (Fig. 1b) were subjected to RNA-seq analysis, and the

overall gene expression profiles are shown in Supplementary Table S4. In NRC rats, we monitored the expression profiles of 60 DEGs that were evaluated in the RC protocol as shown in Fig. 3a-d and Supplementary Table S5. Thirty-four of the 60 selected genes demonstrated significant differential expression in NRC cystitis group (Fig. 3e-g, ≥1.1-fold change, $p < 0.05$, adjusted $p \leq 0.1$ vs saline controls; Supplementary Table S5). Among these 34 genes, 15 were significantly upregulated (Fig. 3e), whereas six were significantly downregulated in both protocols (Fig. 3f). We further examined the statistical differences in fold changes between the treatment protocols and regulation type (up/down) using a multivariable regression model. We observed significant coefficients for the main effects of treatment and regulation type, indicating a statistically significant association between fold-change and treatment. Moreover, we observed a significantly enhanced treatment effect of the RC protocol, with significantly higher fold differences between the groups compared to the NRC protocol ($p < 0.001$, RC vs. NRC). We found significant relationships using the regression coefficient between the effect of rechallenge treatment and non-rechallenge treatment (1.5 ± 0.2, *t-statistic* $= 5.5$, $df = 37$, $p < 0.001$). In contrast, several genes involved in the GABAergic pathway, including GABAa-1, GAD1, and GAD2, were significantly downregulated in the RC protocol, whereas they were upregulated in the NRC protocol (Fig. 3g), indicating GABAergic disinhibition following rechallenge in adulthood. Alternatively, Rims4 and Npff, genes associated with synaptic transmission, demonstrated a > 3.5-fold upregulation in RC protocol with < 1.5-fold downregulation in the NRC protocol.

3.6. Validation of nine DEGs in RNA-seq study for RC groups using TaqMan quantitative RT-PCR

We selected seven genes (Arc, Grip2, Notch1, Grin1, Grin2b, Grin2a, and Scn2b) that exhibited robust upregulation and two genes (Gabra1 and Gabra2) that were strongly downregulated in the RC group for further validation. Our RT-PCR analysis showed that among 7 upregulated genes, the relative expressions ($2^{-\Delta CT}$) of Arc ($p < 0.005$ vs controls), Grip2 ($p < 0.005$ vs controls), Notch1 ($p < 0.05$ vs controls), Grin2b ($p < 0.0005$ vs controls), Grin1 ($p < 0.005$ vs controls), and Scn2b ($p < 0.0005$ vs controls) were significantly higher in the cystitis group compared to saline controls (Fig. 4a-b), validating the expression profiles in RNA-seq study. Similarly, the relative expression of Gabra1 ($p < 0.005$ vs. controls) was significantly downregulated in the cystitis group compared to that in the controls (Fig. 4b), confirming the expression profile in the RNA-seq analysis. However, the RNA-seq expression patterns of Gabra2 and Grin2a could not be validated using RT-PCR (Fig. 4b). The log2 fold changes between experimental and control groups for Grin2b (1 ± 0.2), Notch1 (0.8 ± 0.2), Grip2 (1.8 ± 0.4), Arc (2.1 ± 0.3), Grin1 (1.2 ± 0.2), Scn2b (1 ± 0.3), and Gabra1 (-0.93 ± 0.5) genes are shown in Fig. 4c.

3.7. Differential expression of miRNAs in the RVM neurons of cystitis rats compared to saline controls in RC and NRC protocols

RVM SYNs preparations from the cystitis and saline groups in the RC protocol were subjected to miRNA microarray analysis to investigate the effect of zymosan treatment on miRNA expression in RVM neurons. Microarray analysis revealed the differential expression of miRNAs, with 4 miRNAs (−126a-3p,-34a-5p, −27a-3p, and −6215) downregulated and 11 miRNAs (−342-5p, −138–2-3p, −221-3p, −1188-5p, −139-3p, −125a-3p, −7a-2-3p, −187-3p, −653-5p, –323-3p, and −543-3p) upregulated in cystitis rats compared to saline controls (1.4-fold higher or lower vs controls, $p < 0.05$ vs controls, (Fig. 5a, Supplementary Table S6)). Small-seq analysis of the effect of cystitis in the NRC protocol also identified 8 upregulated and 17 downregulated miRNAs in the neonatal cystitis group ($p < 0.05$ vs controls, (Supplementary, Fig. S1)).

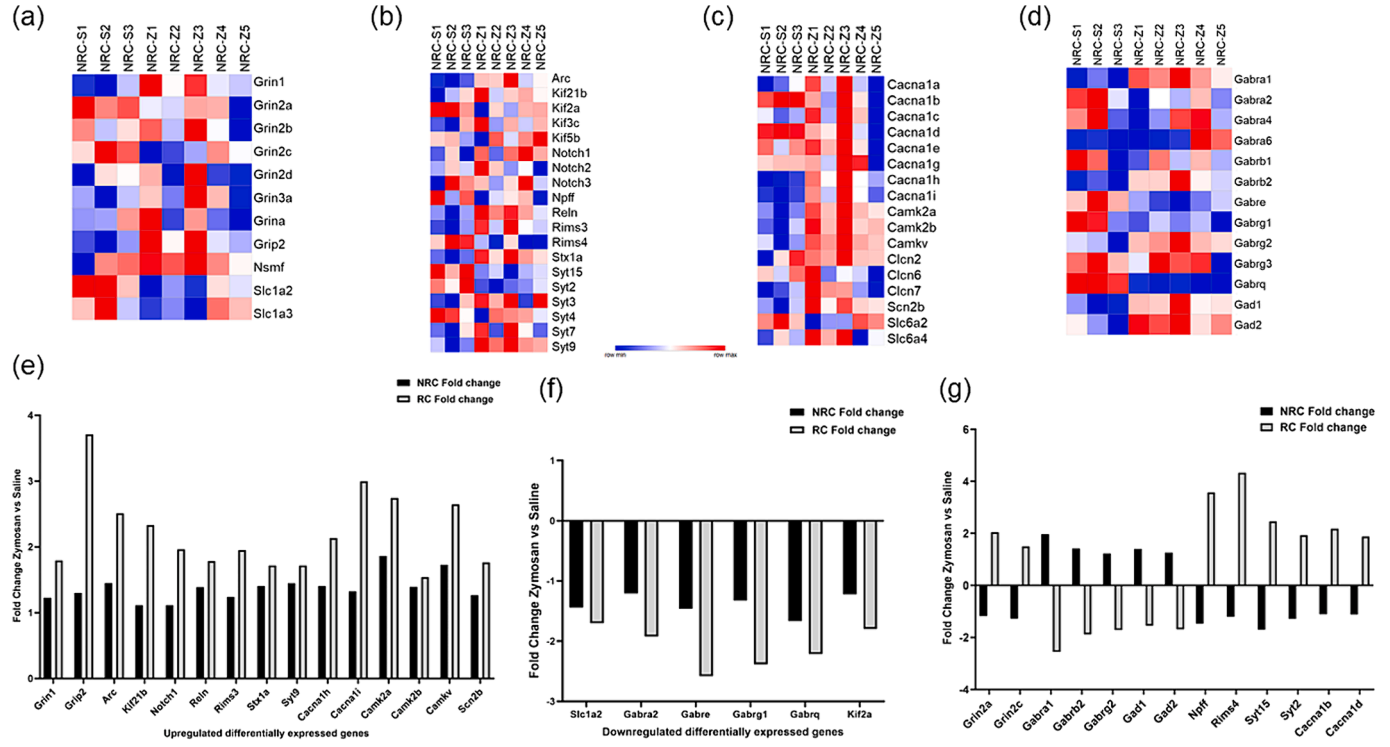

Fig. 3. RNAseq analysis of RVM samples from NRC protocol 2. Heatmaps showing the effect of NRC treatment on the expression profiles of 60 selected genes found to be differentially expressed in RC protocol 1 as shown in Fig. 2. RVM SYNs preparations from neonatal cystitis rats (n = 5) and saline controls (n = 3) were subjected to RNAseq. Heatmaps of genes involved in the glutamatergic pathway (**a**), synaptic plasticity (**b**), voltage-gated calcium/sodium channels and calcium signaling (**c**) and GABAergic pathway (**d**). Among the 60 selected genes found to be differentially expressed in the RC protocol, 34 were differentially expressed in neonatal cystitis rats in the NRC protocol (**e-g**, ≥1.1-fold difference, $p \leq 0.05$ and adjusted $p \leq 0.1$ vs controls). The fold changes in the expression are shown for genes upregulated in both RC and NRC cystitis groups (**e**), genes downregulated in both protocols (**f**), and genes with opposite fold differences in RC and NRC protocols (**g**).

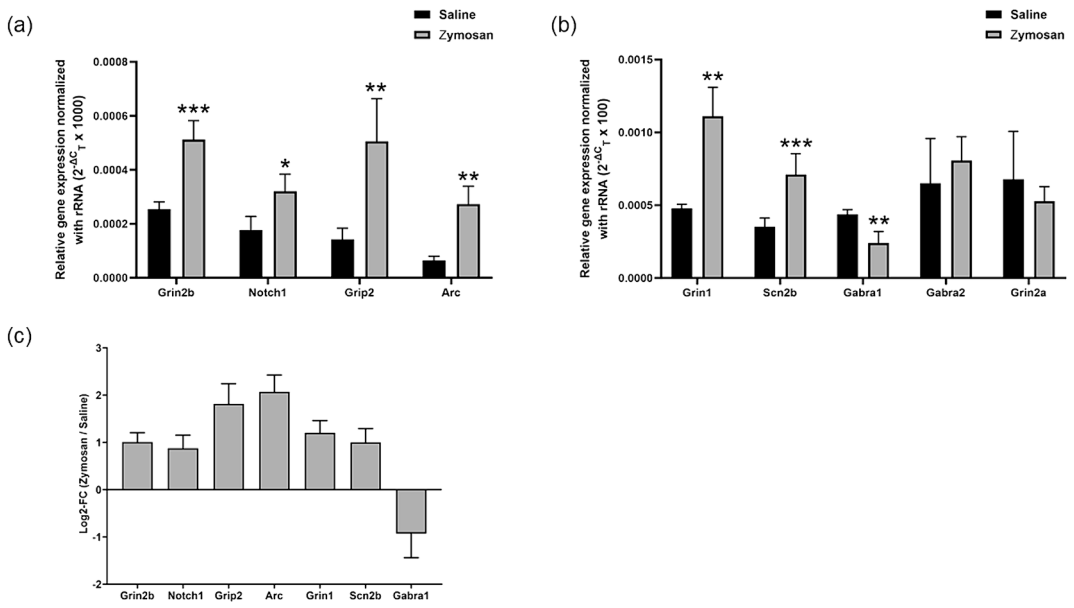

Fig. 4. Validation of the RNAseq results using TaqMan quantitative RT-PCR. Nine DEGs in the RC protocol were selected for further validation by quantitative RT-PCR in the cystitis (n = 5) and saline control (n = 4) groups. Relative gene expressions normalized against the housekeeping 18S gene and presented as $2^{-\Delta C}_{T}$. Data are presented as the mean ± SD (*$p < 0.05$, **$p < 0.01$ and ***$p < 0.001$ vs controls). Unpaired *t*-test with Welch's correction was applied to compare the data between the groups (**a-b**). Relative fold change of differentially expressed genes in cystitis group compared to saline controls (**c**). The Y-axis represents the log2 of fold change of $2^{-\Delta\Delta C}_{T}$ zymosan (cystitis)/saline groups. Data represented as mean ± SD.

Importantly, among the differentially expressed miRNAs, miR-34a-5p and miR-126a-3p were significantly downregulated in the RVM of rats with cystitis in both protocols. (Fig. 5a, Supplementary, Fig. S1, and Supplementary Table S7).

IPA revealed the involvement of the differentially expressed miRNAs in various diseases/functions, including neurological diseases, cell growth and proliferation, inflammatory response, cell-to-cell signaling/interaction, and cell morphology (Fig. 5b; Supplementary Table S8). In particular, the miRNAs,-34a-5p, −27a-3p, and −221-3p were involved in 9 out of 10 identified diseases/functions, whereas −126a-3p was involved in neurological disease, cell growth/proliferation, and cellular function/maintenance, −342-5p in neurological and immunological diseases, and 129-5p in cellular death/survival and cellular growth/proliferation (Fig. 5b; Supplementary Table S8).

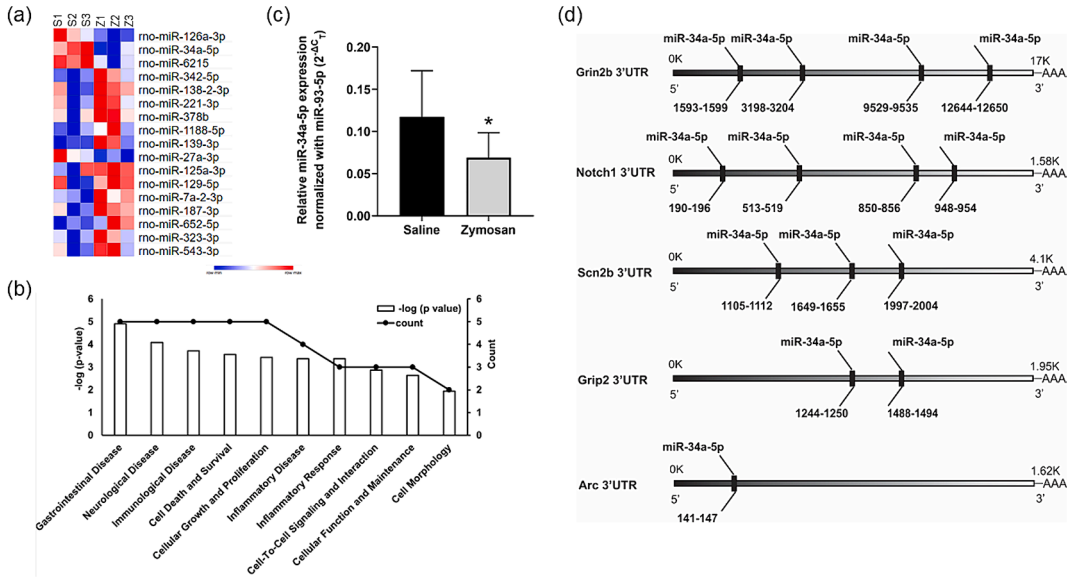

Fig. 5. Effect of cystitis on miRNA expression in RVM. Microarray analysis of miRNA expression in RVM tissues of rats in RC protocol. Heatmap for differentially expressed miRNAs in cystitis rats compared to saline controls (≥1.5-fold difference, $p \leq 0.05$ between the groups), n = 3/group (**a**). Histogram of IPA analysis of differentially expressed miRNAs showing the involvement in 10 functions/diseases (**b**). The left y–axis represents the –log (P–value) and the right y–axis represents the number of miRNAs involved in each disease/function. TaqMan RT-PCR validation of differentially expressed miR-34a-5p in cystitis rats as compared to controls (**c**). Relative miR-34a-5p expression was presented as average $2^{-\Delta C}_{T}$ normalized values against miR-93-5p. Data represented as mean ± SD (n = 5/per group). Unpaired *t*-test with Welch's correction was applied to compare the data between the groups (*$p < 0.05$ vs controls). Bioinformatics analysis revealed multiple complementary binding sites for miR-34a-5p seed region on 3′ UTRs of target genes Grin2b, Notch1, Scn2b, Grip2 and one complementary binding site for 3′UTR of Arc (**d**).

3.8. Bioinformatics analyses and validation of differentially expressed miR-34a-5p

A recent systematic analysis of miRNA expression in the mouse brain using microarray and real-time RT-PCR revealed a six-fold higher expression of miR-34a-5p in the spinal cord, brainstem medulla oblongata, and pons than in the whole mouse brain, indicating its involvement in fine-tuning the expression of various target genes in these specific brain regions (Bak et al., 2008). In agreement with this finding, the microarray analysis in this study showed a very high signal intensity for miR-34a-5p expression in rat midbrain RVM preparations (Supplementary Table S6). Due to its potential involvement in pain pathways and high abundancy in the RVM, we further validated miR-34a-5p expression in RVM SYNs of cystitis and control rats in RC protocol using RT-PCR. The $2^{-\Delta C}_{T}$ values indicated significant downregulation of miR-34a-5p expression in cystitis rats: (0.069 ± 0.02 vs 1.17 ± 0.05, $p < 0.05$ vs controls (Fig. 5c)). Bioinformatic analysis revealed that the downregulated miR-34a-5p carries multiple complementary binding sites for the 3′UTR regions of five DEGs; Grin2b (NR2B subunit of NMDA receptor), Notch1, Grip2, Scn2b and Arc which showed upregulation in RNA-seq analysis (Fig. 5d; Supplementary Fig. S2). The mRNA/miRNA interaction for miR-34a-5p and its target genes Grin2b, Notch1and Arc were also confirmed in several recent studies using 3′UTR gene constructs and luciferase reporter assays (Kern et al., 2021; Pan et al., 2022; Wibrand et al., 2012). In addition, several other DEGs in RNA-seq analysis that are associated with synaptic neurotransmission including Notch2, Notch3, Reln, RIMS3, Cacn1a also carry multiple complementary 3'UTR binding sites for miR-34a-5p (Supplementary Table S9).

3.9. miR-34a-5p colocalizes with targets NR2B (NMDA receptor subunit 2B), Notch1 and Arc in different RVM subnuclei

HCR (ISH)/IHC analysis of miR-34a-5p revealed distinct expression in the RMg and NGc nuclei of the RVM in naïve rats (Fig. 6a). The specificity of miR-34a-5p expression in the RVM was confirmed using a negative control probe for the HCR analysis (Fig. 6b). We further evaluated the co-expression of miR-34a-5p with the NMDA receptor subunit NR2B (Fig. 6c), synaptic protein Notch1 (Fig. 6d), and Arc (Fig. 6e) using dual HCR/IHC. Higher magnification imaging showed distinct co-expression of miR-35a-5p and NR2B in the subnuclei of the RMg (Fig. 6f) and NGc (Fig. 6g). The percentage of miR-34a-5p positive neurons expressing NR2B, Notch1 and Arc in pain relevant RMg and NGc subnuclei of RVM neurons are 73 ± 11.4, 52.2 ± 24, 73 ± 9.8 respectively (Fig. 6h).

3.10. Co-expression of NR1 with NR2B, Notch1 and Arc in RVM neurons

The differentially expressed genes validated by RT-PCR were further

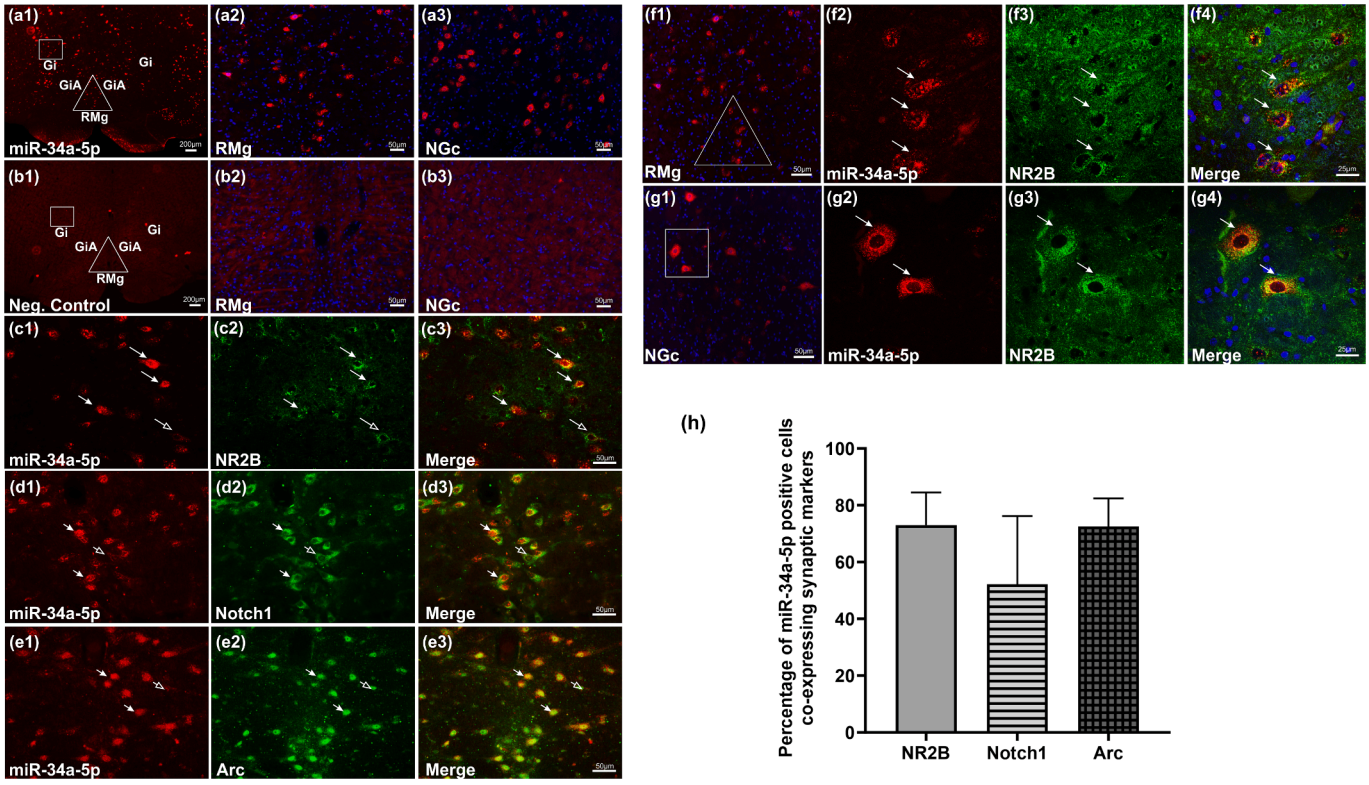

Fig. 6. miR-34a-5p is co-expressed with target genes in RVM neurons. Dual HCR/IHC stainings using a miR-34a-5p probe, followed by antibodies for IHC (naïve rats, n = 3, 3 sections/rat). Representation of miR-34a-5p expression showing RVM nuclei selected for analysis (**a1**). The scale bar is 200 μm. The triangle represents the Raphe Magnus (RMg) sub-nucleus, and the square represents the NGc (Gi/GiA) sub-nuclei. Positive staining for cells/neurons were examined in both sides and higher magnification images of miR-34a-5p expression are shown along with DAPI in RMg (**a2**) and NGc (**a3**). Scale bar is 50 μm. A representation of the negative control probe to confirm the specificity of miR-34a-5p staining in RVM sub-nuclei is shown in (**b1**). The scale bar is 200 μm. Higher magnification images of negative control probe are shown in RMg (**b2**) and NGc (**b3**). Representative images of RVM tissue section (RMg) showing co-expression of miR-34a-5p and its target NR2B (**c1-c3**). Representative images showing the co-expression of miR-34a-5p and its target Notch1 in RVM (RMg) tissues (**d1-d3**). Representative images showing the co-expression of miR-34a-5p and its target anti-Arc in RVM (RMg) tissues (**e1-e3**). The scale bar is 50 μm. Filled white arrows represent miR-34a-5p co-expressing NR2B, Notch1, and Arc whereas hollow arrows represent miR-34a-5p positive cells without NR2B, Notch1, and Arc staining. Higher magnification confocal images of the selected area in (f1) showing the co-expression of miR-34a-5p and NR2B in the RMg (**f2-f4**). Higher magnification confocal images of the selected area in (g1) showing miR-34a-5p and NR2B co-expression in the NGc (**g2-g4**). The scale bar is 25 μm. Filled white arrows represent miR-34a-5p co-expression with NR2B. Analytical plot showing percentage colocalization of miR-34a-5p positive cells with NR2B, Notch1, and Arc in RVM neurons (**h**). Data are presented as the mean ± SD, (n = 3, 3 sections/rat).

evaluated for their expression profiles in the RVM neurons of naïve rats using IHC (Fig. 7a). NR1 expression (the obligatory subunit of all NMDA receptors) was used as a marker for glutamatergic neurons, and NR1 co-expression with NR2B, Notch1, and Arc was further examined in RVM tissues (Fig. 7a). Because the RMg and NGc subnuclei of the RVM are involved in glutamate-mediated facilitatory responses, we focused on evaluating the percentage of NR1 positive neurons expressing the validated genes associated with glutamatergic neurotransmission in these regions of the RVM. The percentage of NR1 positive neurons co-expressing NR2B, Notch1 and Arc in the RVM were 82.4 ± 8.8, 73.5 ± 8.3 and 56.4 ± 16.6, respectively (Fig. 7b).

3.11. Induction of cystitis upregulates the expression of NMDA receptor subunit NR2B in RVM

To further examine the effect of zymosan rechallenge on the NMDA receptor subunits NR1 and NR2B protein expression in the RVM neurons of cystitis rats, we performed IHC on RVM tissue sections from the cystitis and saline groups in the RC treatment protocol (Fig. 8a). IHC quantitative analysis revealed that the intensity of NR2B staining is significantly higher in cystitis rats ($p < 0.05$ vs saline controls; (Fig. 8b), whereas NR1 expression showed a similar trend in cystitis rats; however, no significant difference was observed between the cystitis and control groups.

4. Discussion

In the present study, we investigated the molecular alterations in RVM neurons following neonatal zymosan exposures in rats with or without rechallenge in adulthood. We carried out a thorough investigation to identify the long-term molecular changes, if any, in RVM neurons due to early life bladder exposures to zymosan and evaluated whether rechallenge in adulthood exacerbates the underlying molecular responses due to the priming effect of prior exposures during development. Unbiased high-throughput whole-genome sequencing of the synaptoneurosome preparations from RVM tissues in both protocols revealed the differential expression of several synapse-associated genes, including receptors, voltage-gated channels, and transporters, in the cystitis groups compared to the respective saline controls. Our results further indicated that among the selected 60 DEGs in adult rechallenge protocol, 34 genes also exhibited differential expression in NRC protocol with only early life exposures, indicating comparable molecular processing and synaptic plasticity in both NRC and RC treatment conditions. However, the changes in RVM samples of the RC protocol are more robust, suggesting that acute re-exposure in adulthood exaggerates the underlying molecular alterations of early life zymosan exposures. These findings may explain the molecular mechanisms of the long-term neuronal sensitization related to an overactive bladder or hyperexcitation of spinal neurons to urinary bladder distension, as observed in neonatal-induced cystitis (Kannampalli et al., 2017; Miranda et al., 2011) and hypersensitivity following re-exposure to inflammatory stimuli in adulthood (DeBerry et al., 2007; DeBerry et al., 2010; Randich et al., 2006).

Accumulating evidence indicates the involvement of NMDA receptor subunits in glutamatergic neurotransmission within the RVM (Urban et al., 1999). Specifically, microinjection of NMDA antagonists into the RVM blocks visceral hypersensitivity (Coutinho et al., 1998), mustard oil–induced hypersensitivity (Urban et al., 1999), and neuropathic hypersensitivity (Wei & Pertovaara, 1999). Similarly, in animal model of repeated acidic saline-induced chronic muscle pain, overexpression of the NMDA receptor subunit NR1 in the RVM reduced cutaneous and muscle withdrawal thresholds, indicating somatic hyperalgesia (Da Silva et al., 2010b). It has previously been shown that the RMg and NGc are key nuclei within the RVM that mediate descending facilitation following noxious stimuli and microinjection of low doses of glutamate into the RMg also reported to facilitate pain (Da Silva et al., 2010a; Zhuo & Gebhart, 1992; Porreca et al., 2002). Our IHC analysis demonstrated a significant increase in expression of the NMDA receptor subunit NR2B in the RMg and NGc of glutamatergic RVM neurons of cystitis rats compared to saline controls, emphasizing a possible enhancement of excitatory neurotransmission with cystitis-mediated upregulation of NMDA receptor subunit NR2B in RVM neurons. Although most of our basic knowledge of the midbrain spinal pathway is derived from experimental animal models, recent human studies have also implicated brainstem and spinal cord fMRI activation patterns in pain modulation (Mills et al., 2021). The major limitation of the present study is the lack of behavioral and functional implications of these molecular changes on bladder pain mechanisms. Future studies will be designed to investigate the effects of pharmacological and siRNA-based molecular targeting of NMDA receptor subunits on bladder pain responses in experimental models of cystitis.

Noncanonical Notch1 signaling is highly active in mature neurons, and conditional disruption studies have shown that Notch1 is required for normal spine morphology. Moreover, the activity-regulated gene, Arc, is reported to regulate the proteolytic processing of Notch1, and positively influences Notch signaling in hippocampal neurons (Alberi et al., 2011). In the conditional Notch1-Knockout postnatal hippocampus, the reduction in LTP and LTD, which underlie NMDA functions, further establishes Notch1 dependent regulation of glutamatergic signaling in neurons (Brai et al., 2015). Several recent studies also implicated Notch1 and voltage gated sodium channel Scn2b in mechanical allodynia as well as in the induction and maintenance of neuropathic pain (Pertin et al., 2005; Xie et al., 2015). In line with these findings, the significant upregulation of Notch1, Arc, Scn2b, NR1, and NR2B genes in RVM of cystitis rats in the present study also emphasized their potential involvement in overall excitatory glutamatergic neurotransmission and bladder pain processing. Moreover, our RNAseq analysis showed upregulation of several VGCCs and active zone proteins in the RVM of cystitis rats, with distinctly higher changes in the RC protocol compared to the NRC protocol, indicating a potential priming effect of early life zymosan exposures on calcium channel function later in adulthood. VGCCs and active zone proteins are the dominant contributors to synaptic transmission and are central in regulating the probability of neurotransmitter release in presynaptic active zones (Cunningham & Littleton, 2022; Dolphin & Lee, 2020). Taken together, our findings indicate that cystitis-induced alterations in the expression of various VGCCs and related active zone proteins may profoundly affect the strength of synaptic neurotransmitter output in the RVM and could play a critical role in bladder hypersensitivity.

The specific involvement of miRNAs in visceral nociception through the deregulation of neurotransmitters, receptors, and transporters has been established in animal models, as well as in human visceral pain disorders, including BPS/IC (Gheinani et al., 2021; Monastyrskaya et al., 2013; Sanchez Freire et al., 2010). Our recent studies implicated spinal miRNAs in long-term bladder hypersensitivity in rats with early life cystitis (Sengupta et al., 2013; Zhang et al., 2017). These studies demonstrated an increase in spinal miR-181a and miR-92b-3p with concomitant down-regulation of their targets $GABA_{A\alpha\text{-}1}$ receptor subunit, potassium chloride co-transporter KCC2, and GABA vesicular transporter VGAT gene expression in spinal dorsal horn neurons. Furthermore, behavioral studies have shown that the intrathecal administration of a lentiviral miR-92b-3p sponge significantly attenuated the VMR responses in rats with cystitis, emphasizing the critical involvement of miRNA-mediated molecular alterations in the development of chronic bladder pain conditions associated with cystitis (Zhang et al., 2017). In the present study, we further investigated the possible miRNA-mediated transcriptional deregulation in RVM neurons following cystitis. Among the identified differentially expressed miRNAs, miR-34a-5p, which is highly expressed in the brainstem RVM, was significantly downregulated in the cystitis groups in both the RC and NRC protocols compared to their respective controls. Moreover, bioinformatic analysis for miR-34a-5p targets revealed that five

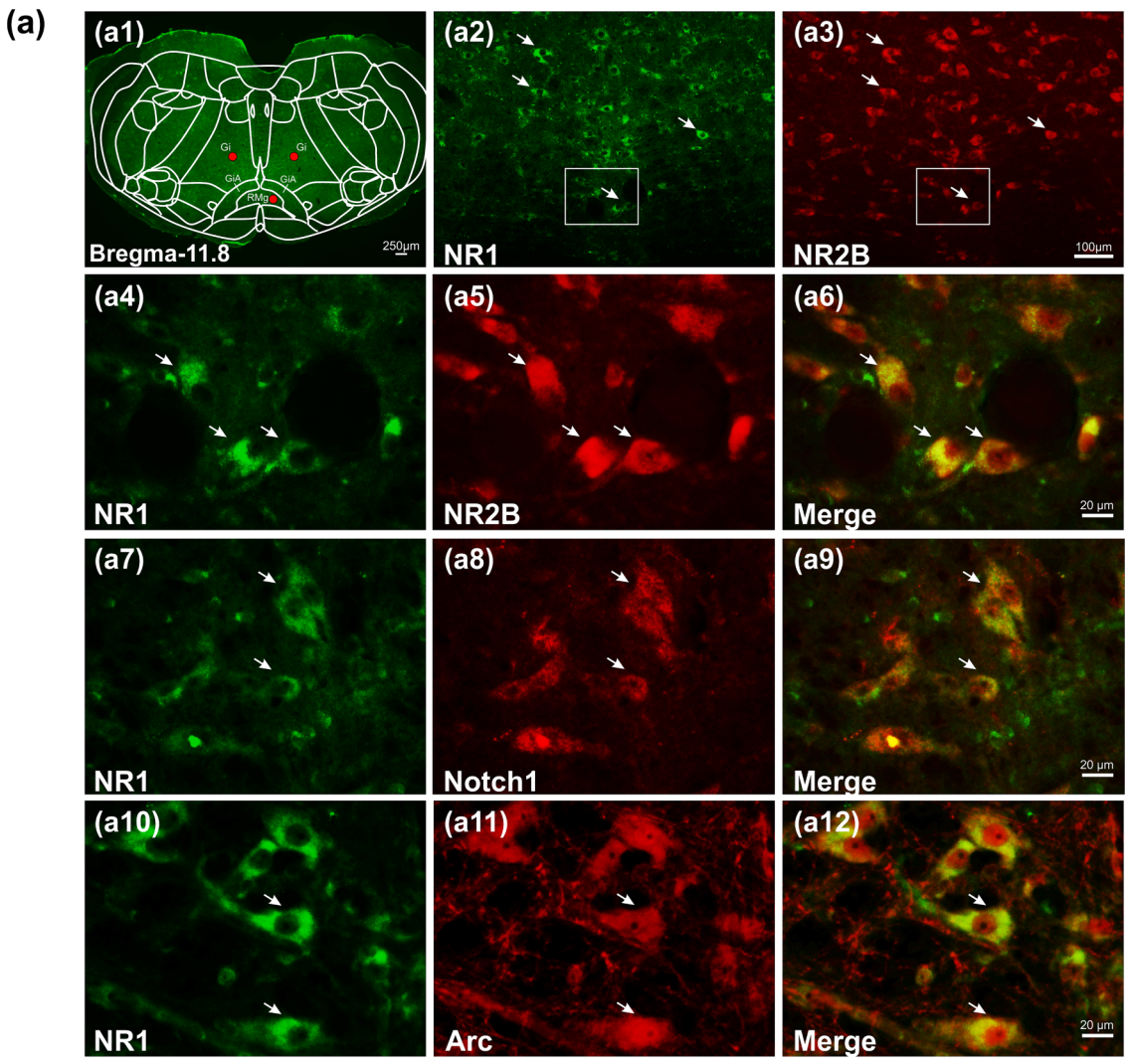

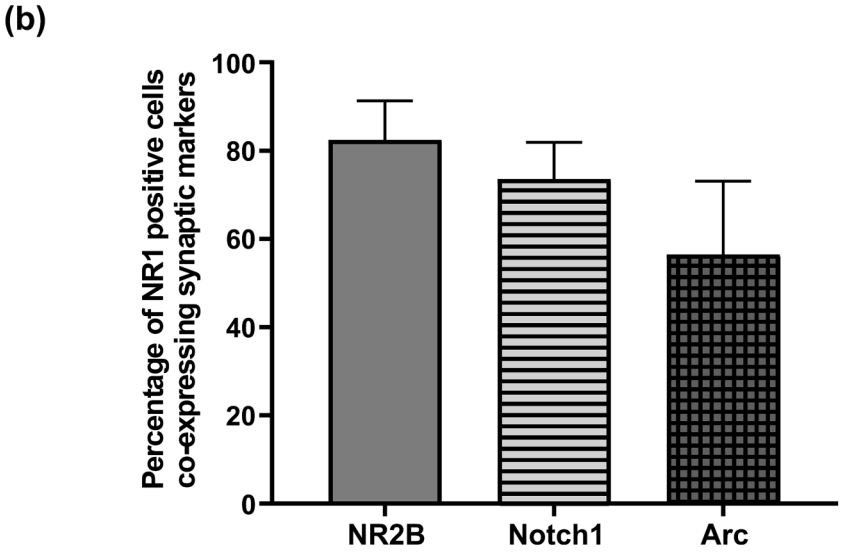

Fig. 7. NR1 positive RVM neurons co-expressed with NR2B, Notch1, and Arc. Representative RVM section at bregma − 11.88 mm, showing the NR1 expression pattern in various RVM sub-nuclei (**a1**). The scale bar is 250 μm. Lower magnification images of NR1 and NR2B expression in RVM (**a2-a3**). The scale bar is 100 μm. A higher magnification of the selected area representing RMg subnuclus in (**a2-a3**) showing the co-expression of NR1 with NR2B (**a4-a6**), Notch1 (**a7-a9**), and Arc (**a10-a12**) within the RVM. White arrows indicate colocalization of NR1 with NR2B (**a6**), Notch1 (**a9**) and, Arc (**a12**). The scale bar is 20 μm. Analytical plot showing the percentage colocalization of NR1 positive cells with NR2B, Notch1, and Arc in RVM neurons (**b**). Data are presented as the mean ± SD, (n = 3, 3 sections/rat).

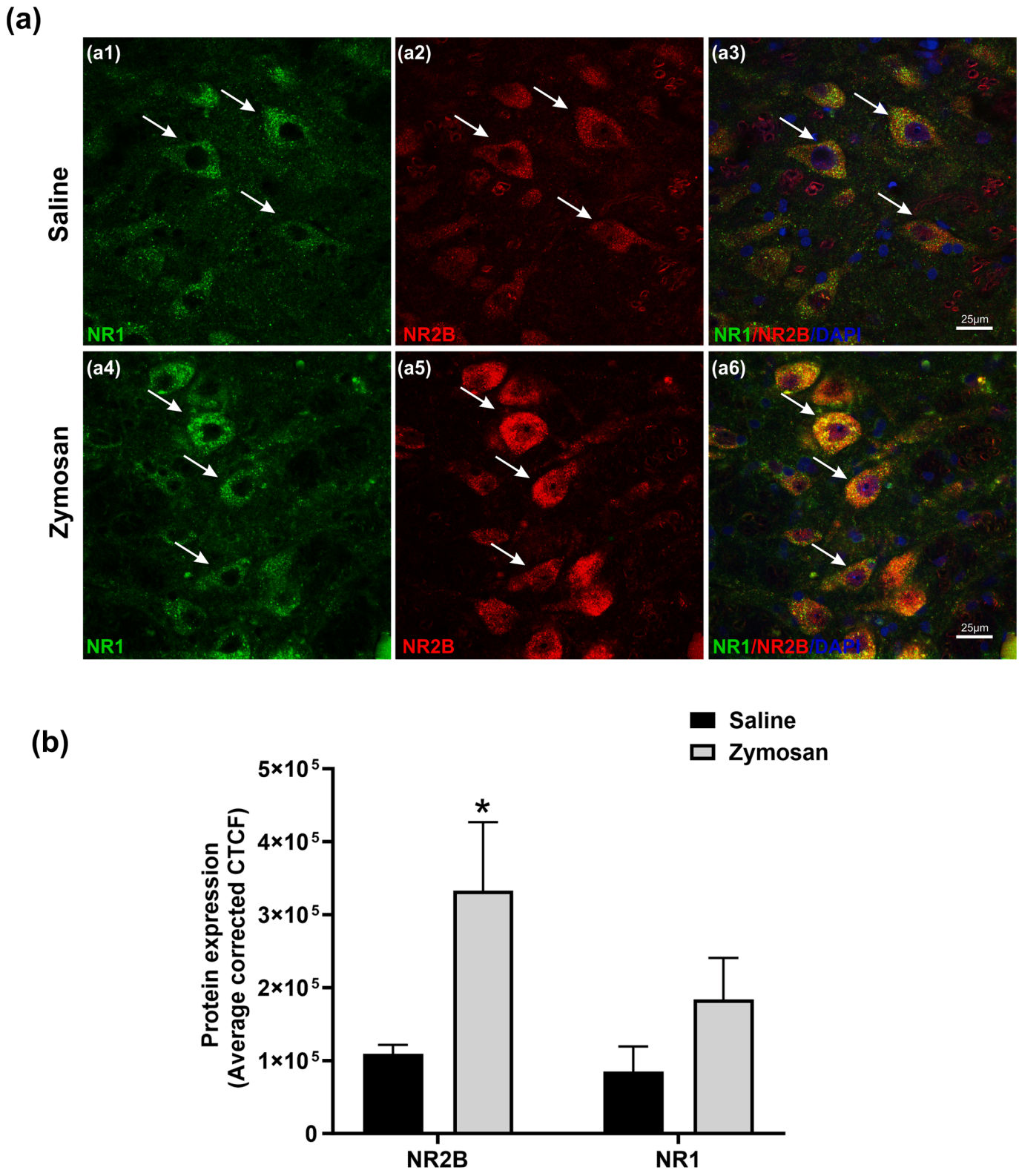

Fig. 8. Induction of cystitis upregulates the expression of the NMDA receptor subunit NR2B in the RC protocol. Expression profile of NR1 and NR2B in the RVM neurons of saline (**a1-a3**) and zymosan-treated cystitis rats (**a4-a6**). The higher magnification confocal imaging shows the co-expression of NR1 and NR2B (white arrows). The scale bar is 25 μm. Analytical plot showing the average intensity of staining measured as Corrected Total Cell Fluorescence (CTCF) of NR2B and NR1 in saline vs zymosan treated cystitis rats (**b**). Data are presented as the mean ± SD (n = 3/group, 3 sections/rat). Unpaired *t*-test with Welch's correction was applied to compare the data between groups (*$p \leq 0.05$ vs controls).

upregulated genes in cystitis rats (Notch1, Grin2b, Grip2, Arc and Scn2b) carry one or more 3′UTR complementary binding sites for the seed region of miR-34a-5p. In support of our findings, several recent studies using luciferase reporter gene assays have confirmed that Notch1, Arc, Scn2b, and Grin2b are validated targets of miR-34a-5p (Kern et al., 2021; Pan et al., 2022; Wibrand et al., 2012). Moreover, in transgenic mice, conditional overexpression of miR-34a-5p triggered rapid cognitive impairment and significant downregulation of the target genes ADAM10, NMDAR subunit NR2B, and SIRT1 in several brain regions, including the hippocampus, thalamus, and prefrontal cortex, indicating the critical role of miR-34a-5p as a regulator of synaptic neurotransmission in the CNS (Sarkar et al., 2019). In experimental model of TNBS-induced ulcerative colitis, miR-34a-5p reported to regulate the antinociceptive effect by targeting the transcription factor HDAC2 (Liang et al., 2019). The downregulation of miR-34a-5p has also been implicated in anti-inflammatory and neuroprotective processes in neuropathic pain model (Brandenburger et al., 2019). Although we demonstrated co-expression of miR-34a-5p and several of its target genes associated with synaptic neurotransmission in the pain relevant RMg and NGc nuclei of RVM, future behavioral studies using site specific lentiviral miR-34a-5p mimic manipulation strategies will confirm its role in altered descending pain modulation following induction of cystitis.

In summary, the present study delineated the long-term molecular changes in RVM neurons with early in-life bladder inflammation, confirming that adult rechallenge exacerbates the underlying molecular responses because of the priming effect of prior exposures during neuronal development. A detailed analysis further revealed the significant upregulation of several genes associated with glutamatergic neurotransmission, including the NMDA receptor subunits NR1 and NR2B, in rats with cystitis. We also demonstrated that miRNAs were differentially expressed in RVM neurons in response to long-term bladder sensitization following cystitis induction. Specifically, miR-34a-5p, which is abundantly expressed in the midbrain, was significantly downregulated, an effect which occurred concomitantly with the upregulation of several target genes, including GRIN2B, Notch1, and Scn2b, indicating the possible involvement of miRNA-mediated transcriptional deregulation of glutamatergic neurotransmission in rats with cystitis compared to controls. Recently, several miRNAs were found to induce analgesia or hypersensitivity in animal models by targeting various pathways associated with neuronal excitability and inflammation. Therefore, the identification of differentially expressed RVM miRNAs in our model of cystitis is critical step forward to develop a better understanding of the pathophysiology of bladder pain and several other overlapping visceral pain conditions that share common neuronal pathways. The direct functional implications of the molecular alterations in RVM cannot be determined from the present data, these findings nevertheless provide crucial information about the molecular mechanisms underlying bladder pain syndrome, and future research will define the significance and possible therapeutic potential of this mechanism.

CRediT authorship contribution statement

Bhavana Talluri: Writing – original draft, Visualization, Validation, Methodology, Investigation, Formal analysis, Data curation. **Sankar Addya:** Writing – review & editing, Visualization, Validation, Supervision, Methodology, Formal analysis, Data curation. **Maia Terashvili:** Methodology, Investigation. **Bidyut K Medda:** Methodology, Investigation. **Anjishnu Banerjee:** Writing – review & editing, Software, Formal analysis. **Reza Shaker:** Writing – review & editing, Resources. **Jyoti N Sengupta:** Writing – review & editing, Resources, Funding acquisition. **Banani Banerjee:** Writing – review & editing, Validation, Supervision, Resources, Project administration, Investigation, Funding acquisition, Conceptualization.

Declaration of competing interest

The authors declare that they have no known competing financial interests or personal relationships that could have appeared to influence the work reported in this paper.

Data availability

Data will be made available on request.

Acknowledgements

This study was supported by the National Institute of Health (NIH) 2R01DK099201-05 grant. This work was supported in part by the NIH shared equipment grant S10OD032136 for Confocal imaging at the CVC Microscopy Core of the Medical College of Wisconsin.

Appendix A. Supplementary data

Supplementary data to this article can be found online at https://doi.org/10.1016/j.ynpai.2024.100160.

References

Alagiri, M., Chottiner, S., Ratner, V., Slade, D., Hanno, P.M., 1997. Interstitial cystitis: unexplained associations with other chronic disease and pain syndromes. Urology 49 (5A Suppl), 52–57. https://doi.org/10.1016/s0090-4295(99)80332-x.

Alberi, L., Liu, S., Wang, Y., Badie, R., Smith-Hicks, C., Wu, J., Pierfelice, T.J., Abazyan, B., Mattson, M.P., Kuhl, D., Pletnikov, M., Worley, P.F., Gaiano, N., 2011. Activity-induced Notch signaling in neurons requires Arc/Arg3.1 and is essential for synaptic plasticity in hippocampal networks. Neuron 69 (3), 437–444. https://doi.org/10.1016/j.neuron.2011.01.004.

Bak, M., Silahtaroglu, A., Moller, M., Christensen, M., Rath, M.F., Skryabin, B., Tommerup, N., Kauppinen, S., 2008. MicroRNA expression in the adult mouse central nervous system. RNA 14 (3), 432–444. https://doi.org/10.1261/rna.783108.

Banerjee, B., Medda, B.K., Zhang, J., Tuchscherer, V., Babygirija, R., Kannampalli, P., Sengupta, J.N., Shaker, R., 2016. Prolonged esophageal acid exposures induce synaptic downscaling of cortical membrane AMPA receptor subunits in rats. Neurogastroenterol. Motil. 28 (9), 1356–1369. https://doi.org/10.1111/nmo.12834.

Basbaum, A.I., Fields, H.L., 1978. Endogenous pain control mechanisms: review and hypothesis. Ann. Neurol. 4 (5), 451–462. https://doi.org/10.1002/ana.410040511.

Brai, E., Marathe, S., Astori, S., Fredj, N.B., Perry, E., Lamy, C., Scotti, A., Alberi, L., 2015. Notch1 Regulates Hippocampal Plasticity Through Interaction with the Reelin Pathway, Glutamatergic Transmission and CREB Signaling. Front. Cell. Neurosci. 9, 447. https://doi.org/10.3389/fncel.2015.00447.

Brandenburger, T., Johannsen, L., Prassek, V., Kuebart, A., Raile, J., Wohlfromm, S., Kohrer, K., Huhn, R., Hollmann, M.W., Hermanns, H., 2019. MiR-34a is differentially expressed in dorsal root ganglia in a rat model of chronic neuropathic pain. Neurosci. Lett. 708, 134365 https://doi.org/10.1016/j.neulet.2019.134365.

Cohen, S.P., Mao, J., 2014. Neuropathic pain: mechanisms and their clinical implications. BMJ 348.

Coutinho, V.S., Urban, O.M., Gebhart, F.G., 1998. Role of glutamate receptors and nitric oxide in the rostral ventromedial medulla in visceral hyperalgesia. Pain 78 (1), 59–69. https://doi.org/10.1016/S0304-3959(98)00137-7.

Cunningham, K.L., Littleton, J.T., 2022. Mechanisms controlling the trafficking, localization, and abundance of presynaptic Ca(2+) channels. Front. Mol. Neurosci. 15, 1116729. https://doi.org/10.3389/fnmol.2022.1116729.

Da Silva, L.F., Desantana, J.M., Sluka, K.A., 2010a. Activation of NMDA receptors in the brainstem, rostral ventromedial medulla, and nucleus reticularis gigantocellularis mediates mechanical hyperalgesia produced by repeated intramuscular injections of acidic saline in rats. J. Pain 11 (4), 378–387. https://doi.org/10.1016/j.jpain.2009.08.006.

Da Silva, L.F.S., Walder, R.Y., Davidson, B.L., Wilson, S.P., Sluka, K.A., 2010b. Changes in expression of NMDA-NR1 receptor subunits in the rostral ventromedial medulla modulate pain behaviors. Pain 151 (1), 155–161. https://doi.org/10.1016/j.pain.2010.06.037.

DeBerry, J., Ness, T.J., Robbins, M.T., Randich, A., 2007. Inflammation-induced enhancement of the visceromotor reflex to urinary bladder distention: modulation by endogenous opioids and the effects of early-in-life experience with bladder inflammation. J. Pain 8 (12), 914–923. https://doi.org/10.1016/j.jpain.2007.06.011.

DeBerry, J., Randich, A., Shaffer, A.D., Robbins, M.T., Ness, T.J., 2010. Neonatal bladder inflammation produces functional changes and alters neuropeptide content in bladders of adult female rats. J. Pain 11 (3), 247–255. https://doi.org/10.1016/j.jpain.2009.07.010.

Dolphin, A.C., Lee, A., 2020. Presynaptic calcium channels: specialized control of synaptic neurotransmitter release. Nat. Rev. Neurosci. 21 (4), 213–229. https://doi.org/10.1038/s41583-020-0278-2.

Durden, E., Walker, D., Gray, S., Fowler, R., Juneau, P., Gooch, K., 2018. The economic burden of overactive bladder (OAB) and its effects on the costs associated with other chronic, age-related comorbidities in the United States. Neurourol. Urodyn. 37 (5), 1641–1649. https://doi.org/10.1002/nau.23513.

Dweep, H., Gretz, N., 2015. miRWalk2.0: a comprehensive atlas of microRNA-target interactions. Nat. Methods 12 (8), 697. https://doi.org/10.1038/nmeth.3485.

Fritschy, J.M., Brunig, I., 2003. Formation and plasticity of GABAergic synapses: physiological mechanisms and pathophysiological implications. Pharmacol. Ther. 98 (3), 299–323. https://doi.org/10.1016/s0163-7258(03)00037-8.

Gheinani, A.H., Akshay, A., Besic, M., Kuhn, A., Keller, I., Bruggmann, R., Rehrauer, H., Adam, R.M., Burkhard, F.C., Monastyrskaya, K., 2021. Integrated mRNA-miRNA transcriptome analysis of bladder biopsies from patients with bladder pain syndrome identifies signaling alterations contributing to the disease pathogenesis. BMC Urol. 21 (1), 172. https://doi.org/10.1186/s12894-021-00934-0.

Grundy, L., Caldwell, A., Brierley, S.M., 2018. Mechanisms underlying overactive bladder and interstitial cystitis/painful bladder syndrome. Front. Neurosci. 12, 931. https://doi.org/10.3389/fnins.2018.00931.

Heinricher, M.M., Tavares, I., Leith, J.L., Lumb, B.M., 2009. Descending control of nociception: Specificity, recruitment and plasticity. Brain Res. Rev. 60 (1), 214–225. https://doi.org/10.1016/j.brainresrev.2008.12.009.

Johnson, M.W., Chotiner, J.K., Watson, J.B., 1997. Isolation and characterization of synaptoneurosomes from single rat hippocampal slices. J. Neurosci. Methods 77 (2), 151–156. https://doi.org/10.1016/s0165-0270(97)00120-9.

Kannampalli, P., Poli, S.M., Bolea, C., Sengupta, J.N., 2017. Analgesic effect of ADX71441, a positive allosteric modulator (PAM) of GABA(B) receptor in a rat model of bladder pain. Neuropharmacology 126, 1–11. https://doi.org/10.1016/j.neuropharm.2017.08.023.

Kern, F., Krammes, L., Danz, K., Diener, C., Kehl, T., Kuchler, O., Fehlmann, T., Kahraman, M., Rheinheimer, S., Aparicio-Puerta, E., Wagner, S., Ludwig, N., Backes, C., Lenhof, H.P., von Briesen, H., Hart, M., Keller, A., Meese, E., 2021. Validation of human microRNA target pathways enables evaluation of target prediction tools. Nucleic Acids Res. 49 (1), 127–144. https://doi.org/10.1093/nar/gkaa1161.

Liang, M., Shao, A., Tang, X., Feng, M., Wang, J., Qiu, Y., 2019. MiR-34a affects dexmedetomidine-inhibited chronic inflammatory visceral pain by targeting to HDAC2. BMC Anesthesiol. 19 (1), 131. https://doi.org/10.1186/s12871-019-0801-z.

Lim, L.P., Glasner, M.E., Yekta, S., Burge, C.B., Bartel, D.P., 2003. Vertebrate microRNA genes. Science 299 (5612), 1540. https://doi.org/10.1126/science.1080372.

Mills, E.P., Keay, K.A., Henderson, L.A., 2021. Brainstem pain-modulation circuitry and its plasticity in neuropathic pain: insights from human brain imaging investigations. Front Pain Res. (lausanne) 2, 705345. https://doi.org/10.3389/fpain.2021.705345.

Miranda, A., Mickle, A., Schmidt, J., Zhang, Z., Shaker, R., Banerjee, B., Sengupta, J.N., 2011. Neonatal cystitis-induced colonic hypersensitivity in adult rats: a model of viscero-visceral convergence. Neurogastroenterol. Motil. 23 (7), 683–e281. https://doi.org/10.1111/j.1365-2982.2011.01724.x.

Monastyrskaya, K., Sanchez-Freire, V., Hashemi Gheinani, A., Klumpp, D.J., Babiychuk, E.B., Draeger, A., Burkhard, F.C., 2013. miR-199a-5p regulates urothelial permeability and may play a role in bladder pain syndrome. Am. J. Pathol. 182 (2), 431–448. https://doi.org/10.1016/j.ajpath.2012.10.020.

Niederberger, E., Kynast, K., Lotsch, J., Geisslinger, G., 2011. MicroRNAs as new players in the pain game. Pain 152 (7), 1455–1458. https://doi.org/10.1016/j.pain.2011.01.042.

Offiah, I., Campbell, R., Dua, A., Bombieri, L., & Freeman, R. (2022). Present status and advances in bladder pain syndrome: central sensitisation and the urinary microbiome.

Ossipov, M.H., Morimura, K., Porreca, F., 2014. Descending pain modulation and chronification of pain. Curr. Opin. Support. Palliat. Care 8 (2), 143–151. https://doi.org/10.1097/SPC.0000000000000055.

Pan, J., Zhou, L., Lin, C., Xue, W., Chen, P., Lin, J., 2022. MicroRNA-34a promotes ischemia-induced cardiomyocytes apoptosis through targeting notch1. Evid. Based Complement. Alternat. Med. 2022, 1388415. https://doi.org/10.1155/2022/1388415.

Peng, B., Jiao, Y., Zhang, Y., Li, S., Chen, S., Xu, S., Gao, P., Fan, Y., Yu, W., 2023. Bulbospinal nociceptive ON and OFF cells related neural circuits and transmitters. Front. Pharmacol. 14, 1159753. https://doi.org/10.3389/fphar.2023.1159753.

Pertin, M., Ji, R.R., Berta, T., Powell, A.J., Karchewski, L., Tate, S.N., Isom, L.L., Woolf, C. J., Gilliard, N., Spahn, D.R., Decosterd, I., 2005. Upregulation of the voltage-gated sodium channel beta2 subunit in neuropathic pain models: characterization of expression in injured and non-injured primary sensory neurons. J. Neurosci. 25 (47), 10970–10980. https://doi.org/10.1523/JNEUROSCI.3066-05.2005.

Pichardo-Casas, I., Goff, L.A., Swerdel, M.R., Athie, A., Davila, J., Ramos-Brossier, M., Lapid-Volosin, M., Friedman, W.J., Hart, R.P., Vaca, L., 2012. Expression profiling of synaptic microRNAs from the adult rat brain identifies regional differences and seizure-induced dynamic modulation. Brain Res. 1436, 20–33. https://doi.org/10.1016/j.brainres.2011.12.001.

Pierce, A.N., Christianson, J.A., 2015. Stress and chronic pelvic pain. Prog. Mol. Biol. Transl. Sci. 131, 509–535. https://doi.org/10.1016/bs.pmbts.2014.11.009.

Porreca, F., Ossipov, M.H., Gebhart, G.F., 2002. Chronic pain and medullary descending facilitation. Trends Neurosci. 25 (6), 319–325. https://doi.org/10.1016/s0166-2236(02)02157-4.

Raja, S.N., Sivanesan, E., Guan, Y., 2019. Central sensitization, N-methyl-D-aspartate receptors, and human experimental pain models: bridging the gap between target discovery and drug development. Anesthesiology 131 (2), 233–235.

Randich, A., Uzzell, T., DeBerry, J.J., Ness, T.J., 2006. Neonatal urinary bladder inflammation produces adult bladder hypersensitivity. J. Pain 7 (7), 469–479. https://doi.org/10.1016/j.jpain.2006.01.450.

Randich, A., Mebane, H., DeBerry, J.J., Ness, T.J., 2008. Rostral ventral medulla modulation of the visceromotor reflex evoked by urinary bladder distension in female rats. J. Pain 9 (10), 920–926. https://doi.org/10.1016/j.jpain.2008.05.011.

Sanchez Freire, V., Burkhard, F.C., Kessler, T.M., Kuhn, A., Draeger, A., Monastyrskaya, K., 2010. MicroRNAs may mediate the down-regulation of neurokinin-1 receptor in chronic bladder pain syndrome. Am. J. Pathol. 176 (1), 288–303. https://doi.org/10.2353/ajpath.2010.090552.

Sarkar, S., Engler-Chiurazzi, E.B., Cavendish, J.Z., Povroznik, J.M., Russell, A.E., Quintana, D.D., Mathers, P.H., Simpkins, J.W., 2019. Over-expression of miR-34a induces rapid cognitive impairment and Alzheimer's disease-like pathology. Brain Res. 1721, 146327 https://doi.org/10.1016/j.brainres.2019.146327.

Sengupta, J.N., Pochiraju, S., Kannampalli, P., Bruckert, M., Addya, S., Yadav, P., Miranda, A., Shaker, R., Banerjee, B., 2013. MicroRNA-mediated GABA Aalpha-1 receptor subunit down-regulation in adult spinal cord following neonatal cystitis-induced chronic visceral pain in rats. Pain 154 (1), 59–70. https://doi.org/10.1016/j.pain.2012.09.002.

Tirlapur, S., Birch, J., Carberry, C., Khan, K., Latthe, P., Jha, S., Ward, K., Irving, A., 2017. Management of bladder pain syndrome. Bjog- Int. J. Obstet. Gynaecol. 124 (2), E46–E72.

Urban, M.O., Coutinho, S.V., Gebhart, G.F., 1999. Involvement of excitatory amino acid receptors and nitric oxide in the rostral ventromedial medulla in modulating secondary hyperalgesia produced by mustard oil. Pain 81 (1–2), 45–55. https://doi.org/10.1016/s0304-3959(98)00265-6.

Wei, H., Pertovaara, A., 1999. MK-801, an NMDA receptor antagonist, in the rostroventromedial medulla attenuates development of neuropathic symptoms in the rat. Neuroreport 10 (14), 2933–2937. https://doi.org/10.1097/00001756-199909290-00011.

Wibrand, K., Pai, B., Siripornmongcolchai, T., Bittins, M., Berentsen, B., Ofte, M.L., Weigel, A., Skaftnesmo, K.O., Bramham, C.R., 2012. MicroRNA regulation of the synaptic plasticity-related gene Arc. PLoS One 7 (7), e41688.

Williams, C., Mehrian Shai, R., Wu, Y., Hsu, Y.H., Sitzer, T., Spann, B., McCleary, C., Mo, Y., Miller, C.A., 2009. Transcriptome analysis of synaptoneurosomes identifies neuroplasticity genes overexpressed in incipient Alzheimer's disease. PLoS One 4 (3), e4936.

Xie, K., Qiao, F., Sun, Y., Wang, G., Hou, L., 2015. Notch signaling activation is critical to the development of neuropathic pain. BMC Anesthesiol. 15, 1–7.

Yang, M.H., Huang, J.Y., Chen, S.L., Wei, J.C., 2021. Association of interstitial cystitis/bladder pain syndrome with stress-related diseases: a nationwide population-based study. J. Clin. Med. 10 (23) https://doi.org/10.3390/jcm10235669.

Zeng, Y., Cullen, B.R., 2003. Sequence requirements for micro RNA processing and function in human cells. RNA 9 (1), 112–123. https://doi.org/10.1261/rna.2780503.

Zhang, J., Yu, J., Kannampalli, P., Nie, L., Meng, H., Medda, B.K., Shaker, R., Sengupta, J. N., Banerjee, B., 2017. MicroRNA-mediated downregulation of potassium-chloride-cotransporter and vesicular gamma-aminobutyric acid transporter expression in spinal cord contributes to neonatal cystitis-induced visceral pain in rats. Pain 158 (12), 2461–2474. https://doi.org/10.1097/j.pain.0000000000001057.

Zhuang, P., Zhang, H., Welchko, R.M., Thompson, R.C., Xu, S., Turner, D.L., 2020. Combined microRNA and mRNA detection in mammalian retinas by in situ hybridization chain reaction. Sci. Rep. 10 (1), 351. https://doi.org/10.1038/s41598-019-57194-0.

Zhuo, M., Gebhart, G.F., 1992. Characterization of descending facilitation and inhibition of spinal nociceptive transmission from the nuclei reticularis gigantocellularis and gigantocellularis pars alpha in the rat. J. Neurophysiol. 67 (6), 1599–1614. https://doi.org/10.1152/jn.1992.67.6.1599.